Bioinspiration in light harvesting and catalysis

Andrew H. Proppe[1,2,3,25], Yuguang C. Li[1,3,25], Alán Aspuru-Guzik[1,4,5], Curtis P. Berlinguette[1,6,7,8], Christopher J. Chang[1,9], Richard Cogdell[1,10], Abigail G. Doyle[11], Johannes Flick[12], Nathaniel M. Gabor[1,13], Rienk van Grondelle[1,14], Sharon Hammes-Schiffer[1,15], Shaffiq A. Jaffer[1,16], Shana O. Kelley[2,17], Mario Leclerc[1,18], Karl Leo[1,19], Thomas E. Mallouk[1,20], Prineha Narang[1,12], Gabriela S. Schlau-Cohen[1,21], Gregory D. Scholes[1,11], Aleksandra Vojvodic[1,22], Vivian Wing-Wah Yam[1,23], Jenny Y. Yang[1,24] and Edward H. Sargent[1,3]✉

Abstract | Capturing and converting solar energy into fuels and feedstocks is a global challenge that spans numerous disciplines and fields of research. Billions of years of evolution have allowed natural organisms to hone strategies for harvesting light from the sun and storing energy in the form of carbon–carbon and carbon–hydrogen bonds. Photosynthetic antenna proteins capture solar photons and funnel photoexcitations to reaction centres with high yields, and enzymes catalyze multi-electron reactions, facilitating chemical transformations not yet efficiently implemented using artificially engineered catalysts. Researchers in renewable energy often look to nature to understand the mechanisms at work and, if possible, to explore their translation into artificial systems. Here, we review advances in bioinspiration across the fields of biological light harvesting and chemical energy conversion. We examine how multi-photon and multi-electron reactions in biology can inspire new methods in photoredox chemistry to achieve novel, selective and complex organic transformations; how carbonic-dehydrogenase-inspired design principles enable catalytic reactions such as the conversion of CO_2 into useful products such as fuels; and how concepts from photosynthetic antenna complexes and reaction centres can benefit artificial light-harvesting materials. We then consider areas in which bioinspiration could enable advances in the rational design of molecules and materials, the expansion of the synthetic capabilities of catalysts and the valorization of molecular building blocks. We highlight the challenges that must be overcome to realize these advances and propose new directions that may use bioinspiration to achieve them.

Every hour, the amount of sunlight reaching Earth contains more energy than is used by humans in an entire year[1]. Photosynthesis enables organisms to harvest solar photons and use this energy to drive multi-electron chemistry and form higher carbon products from atmospheric CO_2 (REFS[2,3]). The highest efficiency (for plants) of solar-energy conversion into biomass is ~4.6% for C3 photosynthesis (one of the metabolic pathways for carbon fixation) at 30 °C and 380 ppm of atmospheric CO_2 (REF.[4]). In many ways, this is remarkable, not least because of the low concentration of the CO_2 input to the reaction.

Photosynthesis offers numerous sources of bioinspiration for artificial materials. Light-harvesting antenna supercomplexes in plants and photosynthetic bacteria form long-range energy funnels that route excitons — excited electronic states formed by light absorption by chlorophyll — to reaction centres, where they undergo charge separation into free carriers. The overall efficiency (quantum yield) of this process is, under optimal conditions, near unity[5–8]: that photosynthetic membranes comprised of antenna proteins and their constituent pigments allow excitons to migrate very rapidly over long nanoscale distances indicates they are robust against non-radiative losses, even under very disordered and 'noisy' physiological conditions.

The combination of strongly absorbing pigments, rapid energy transfer of excitons to reaction centres and kinetically controlled excited electronic states with long lifetimes allows for the accumulation of multiple carriers

✉*e-mail: ted.sargent@utoronto.ca*

https://doi.org/10.1038/s41578-020-0222-0

at catalytic sites. Enzymes in photosynthetic organisms that reduce CO_2 or split water have optimized the delivery of multiple energetic electrons to perform chemical transformations. In the field of light-driven chemistry, photoredox catalysis has emerged as a promising platform to realize previously inaccessible chemical transformations. Unlike most photoredox catalysts that require the stepwise absorption of single high-energy photons in order to generate excited states with sufficient energy to perform reactions, biological photocatalytic complexes are able to harvest multiple low-energy photons and use their energy concertedly to carry out multi-electron and multi-proton reactions. In the first section of this Review, we look to the role of such energetic schemes driven and coupled by multiple photons in nature, how they have been successfully applied in homogeneous catalysis and how they may be integrated with photoredox catalysis.

We next turn to catalytic reactions facilitated by enzymes, in which biology has evolved mechanisms and pathways that make use of abundant atmospheric molecules such as CO_2 and N_2 to generate compounds essential to the survival of the organism, such as sugars and ammonia. The selectivity of these transformations is high, and artificially engineered catalysts targeting the same molecules have not reached the same level of catalytic efficiency. Enzymes take advantage of molecular flexibility by tailoring the protein scaffolds surrounding active sites, confining reaction intermediates within extremely small regions and mediating substrate and product delivery and their removal from the active site. By contrast, the best-performing artificial electrocatalysts targeting the synthesis of small molecules from CO_2 are comprised of large catalytic surfaces that make little use either of second-sphere effects or of nanoconfinement.

We then examine light harvesting and long-range energy-transport processes in photosynthetic and artificial systems. Photosynthetic membranes consist of coupled antenna complexes that enable the migration of photoexcitations over long distances, a property coveted by organic photovoltaic (OPV) materials, which notoriously suffer from short diffusion lengths[9–11]. This long-range transport is directed by an energy gradient that funnels a steady stream of photoexcitations to reaction centres in order to catalyze cellular reactions, which is desirable in artificial light-driven catalysts. As the field of OPVs has evolved from binary bulk heterojunction (BHJ) blends to also encompass higher-order (ternary and quaternary) mixtures, we revisit how bioinspiration may play a role in state-of-the-art organic solar cells. We also discuss how design principles of natural light harvesting have been implemented in artificial systems exhibiting long-range energy transport and photocatalytic systems using the antennae effect.

Finally, we offer a perspective on bioinspired materials design — bringing together experimental and theoretical viewpoints from inorganic and organic synthetic chemists, engineers, biologists, materials scientists and physicists — on what we propose as pertinent paths in applying bioinspired concepts to chemistry and materials, and what new methodologies are needed in order to more effectively deploy bioinspiration in these areas.

Multi-electron photochemistry

Z-schemes. Three primary steps are involved in the overall chemistry of photosynthesis: light absorption by antenna complexes and pigment molecules; energy transfer to the reaction centres, where charge separation occurs; and chemical reactions within the reaction centres (such as water splitting). In artificial photocatalytic systems, all three steps are often achieved in a single system with suitable energy levels such that, following photon absorption, an electron in the highest occupied molecular orbital level is photoexcited into the lowest unoccupied molecular orbital, where it may reduce an electron acceptor, while the hole remaining in the highest occupied molecular orbital can oxidize an electron donor. These single-step systems are simple but suffer critical design constraints. For instance, they have a limited operational spectral window, because the energy of the absorbed light must be greater than the difference in redox potentials of the oxidation and reduction reactions, with additional energy required

Author addresses

[1]Canadian Institute for Advanced Research (CIFAR), Bioinspired Solar Energy Program, Toronto, Ontario, Canada.
[2]Department of Chemistry, University of Toronto, Toronto, Ontario, Canada.
[3]The Edward S. Rogers Department of Electrical and Computer Engineering, University of Toronto, Toronto, Ontario, Canada.
[4]Department of Chemistry and Department of Computer Science, University of Toronto, Toronto, Ontario, Canada.
[5]Vector Institute, Toronto, Ontario, Canada.
[6]Department of Chemical and Biological Engineering, The University of British Columbia, Vancouver, British Columbia, Canada.
[7]Department of Chemistry, The University of British Columbia, Vancouver, British Columbia, Canada.
[8]Stewart Blusson Quantum Matter Institute, The University of British Columbia, Vancouver, British Columbia, Canada.
[9]Department of Chemistry, Department of Molecular and Cell Biology, University of California, Berkeley, Berkeley, CA, USA.
[10]Institute of Molecular, Cell and Systems Biology, College of Medical, Veterinary and Life Sciences, University of Glasgow, Glasgow, UK.
[11]Department of Chemistry, Princeton University, Princeton NJ, New Jersey, USA.
[12]John A. Paulson School of Engineering and Applied Sciences, Harvard University, Cambridge, MA, USA.
[13]Laboratory of Quantum Materials Optoelectronics, Department of Physics and Astronomy, University of California Riverside, Riverside, CA, USA.
[14]Faculty of Science, Vrije Universiteit Amsterdam, Amsterdam, The Netherlands.
[15]Department of Chemistry, Yale University, New Haven, CT, USA.
[16]TOTAL American Services, Hopkinton, MA, USA.
[17]Department of Pharmaceutical Sciences, Leslie Dan Faculty of Pharmacy, University of Toronto, Toronto, Ontario, Canada.
[18]Department of Chemistry, Université Laval, Quebec City, Quebec, Canada.
[19]Dresden Integrated Center for Applied Physics and Photonic Materials (IAPP), Technische Universität Dresden, Dresden, Germany.
[20]Department of Chemistry, University of Pennsylvania, Philadelphia, PA, USA.
[21]Department of Chemistry, Massachusetts Institute of Technology, Cambridge, MA, USA.
[22]Department of Chemical and Biomolecular Engineering, University of Pennsylvania, Philadelphia, PA, USA.
[23]Department of Chemistry, The University of Hong Kong, Hong Kong, P. R. China.
[24]Department of Chemistry, University of California, Irvine, CA, USA.
[25]These authors contributed equally: Andrew H. Proppe, Yuguang C. Li

as the driving force for these reactions. For the coupled redox reactions that produce oxygen and hydrogen gas ($2H_2O \rightarrow 4H^+ + O_2$ and $2H^+ \rightarrow H_2$), this limits absorption to energies of ~1.8 eV and higher. It has long been recognized that this restriction compromises the solar-conversion efficiency, especially when large overpotentials are required to drive the catalytic anode and cathode reactions[12]. An additional constraint is that it is impractical to rely on the absorption of ultraviolet light: although it provides the energy needed to activate desirable reactions, the light is also absorbed non-selectively, for example, by solvent.

Rather than relying on a single high-energy absorption event, biology deploys stepwise electron-transfer processes between multiple absorbers in what is known as a 'Z-scheme' (FIG. 1a). In this way, two or more

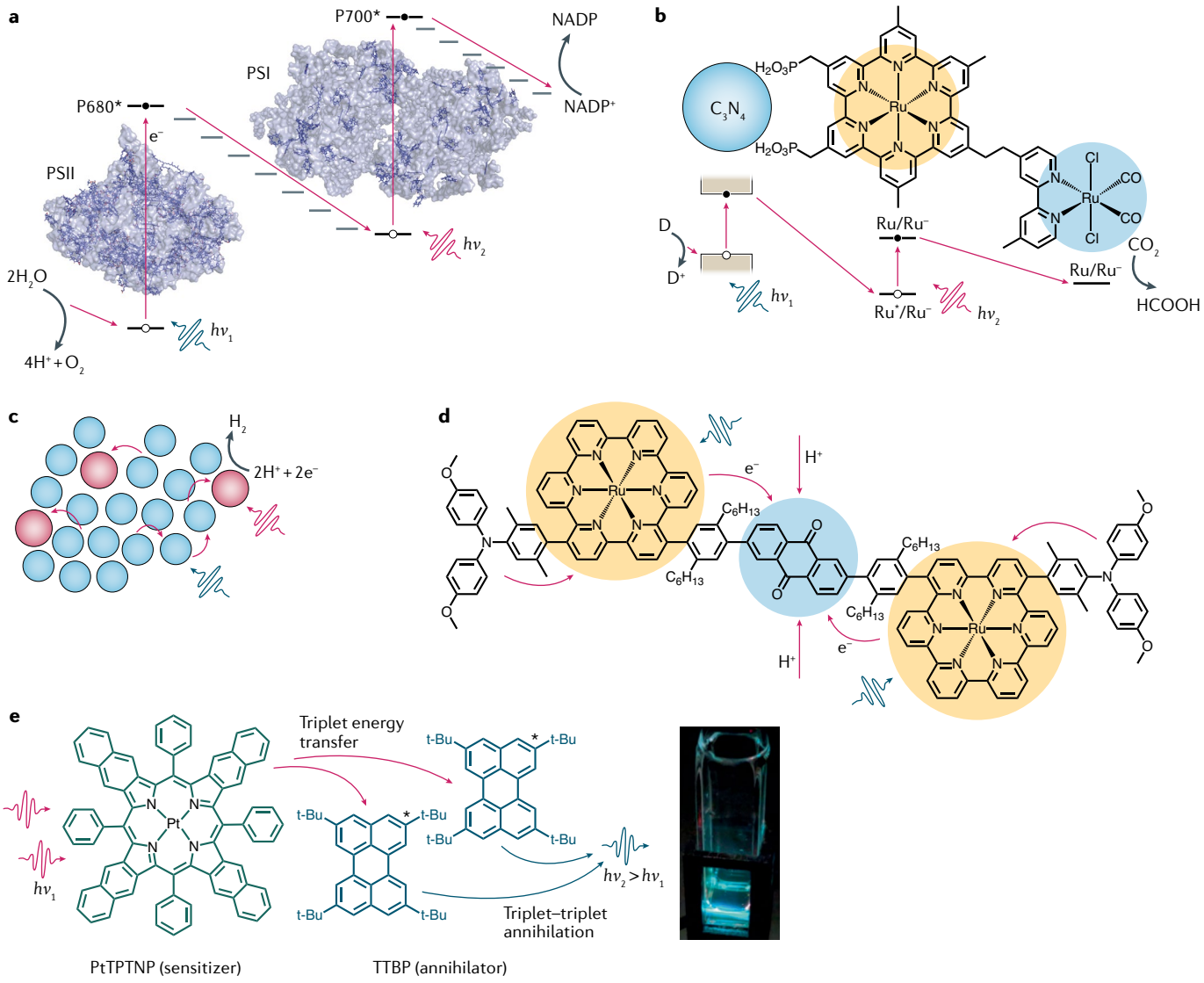

Fig. 1 | **Z-schemes in photocatalysis and multi-electron photochemistry.** **a** | Z-scheme used by photosystem I (PSI) and PSII to drive the water-oxidation reaction and the reduction of NADP. Photoexcited electrons in the absorbing photosystems undergo sequential electron-transfer events through adjacent sites to bridge the reduction of NADP with the oxidation of water (the protein structures are from *Thermosynechococcus elongatus*). P680 and P700 are chlorophylls that absorb light of 680 nm in PSII and 700 nm in PSI, respectively; P680* and P700*are their excited states. **b** | Example of a Z-scheme-driven photocatalytic hybrid system. The ruthenium-absorber chromophore $Ru(bipy)_3$ (yellow) absorbs visible light and donates an excited electron to a nearby ruthenium catalytic active site (blue). A C_3N_4 semiconductor nanoparticle (grey) also absorbs visible light and donates an electron to the oxidized $Ru(bipy)_3$, thereby, forming a photoexcited electron relay to the catalytic active site. A donor molecule (D) provides an electron back to the C_3N_4 nanoparticle. **c** | Assembly of cadmium-selenide quantum dots used to photocatalytically evolve H_2. Photoexcitations generated in wider-bandgap sensitizer dots (blue) undergo sequential energy transfer to smaller-bandgap, catalytically active dots (red). In an optimized 4:1 ratio of sensitizer-to-catalyst quantum dots, the internal quantum efficiency of the reaction is increased 13-fold relative to that of an assembly where energy transfer is suppressed (no funnelling). **d** | Molecular pentad structure that can use visible light to accumulate two electrons on a common acceptor unit[45]. **e** | Annihilators and sensitizers, tetra-*tert*-butylperylene (TTBP) and platinum(II) tetraphenyltetranaphthoporphyrin (PtTPTNP), used in near-infrared-to-blue triplet upconversion photoredox reactions. On the right, a cuvette containing a mixture of PtTPTNP and TTBP is shown to emit blue light under near-infrared photoexcitation. Panel **b** adapted with permission from REF.[13], ACS. Panel **c** adapted with permission from REF.[41], PNAS. Panel **d** adapted with permission from REF.[45], Wiley. Panel **e** adapted from REF.[36], Springer Nature Limited.

lower-energy photons may be used in a series to achieve reactivity of energetically demanding redox couples. Many artificial catalytic systems using Z-schemes have been developed, and an example of such a system is shown in FIG. 1b. By combining a strongly absorbing semiconductor (C_3N_4), a ruthenium-absorber chromophore and a ruthenium catalytic site in a Z-scheme, this system was able to reduce CO_2 to HCOOH with a turnover number (the maximum number of substrate molecules converted to product per active site per unit time) of >30,000 and a selectivity of 99%[13]. A testament to the versatility of the Z-scheme can be seen in the variety of materials used to perform this reaction, such as multi-junction semiconductor electrodes[14,15], multiple-semiconductor particles[16–18], polymeric van der Waals heterostructures[19] and semiconductor–metal complex hybrids[20–24].

It is important to note a distinction between artificial and natural systems that exploit Z-schemes. Biology uses Z-schemes in order to separate light-dependent reactions (those used to form energetic molecules) from dark, or light-independent, CO_2-fixation reactions. By contrast, artificial photocatalytic systems using Z-schemes couple both types of reactions: the energy from the absorbed photons is directly used to make the photoproduct. This represents an example of bioinspiration that does not aim to exactly mimic a biological system or a biological structure but, instead, tries to achieve new functionality (here, multi-photon-driven reactivity) based on a biological mechanism.

Photoredox beyond single-chromophore catalysts. Photoredox catalysis enables a suite of important organic reactions[25–30]. In recent years, the focus has been on expanding the versatility of these reactions by merging photoredox catalysis with transition-metal catalysis, with eminent advances achieved for photoredox catalysts coupled to nickel and copper catalysts[31–33].

A further expansion of the library of reactions and products obtained using photoredox catalysts and dual-catalytic systems, as well as an increase in the efficiency of these reactions, may be achieved through bioinspired augmentations of the photoredox catalyst. Photoredox catalysts are good targets for bioinspired approaches because they rely on spectrally specific light absorption, long excited-state lifetimes and high quantum yields in order to function efficiently. A principal feature of Z-schemes used in photosynthesis is the wide spectrum of excitation wavelengths that can be used to generate excited electrons that drive redox reactions. Conventional photoredox catalysts, typically consisting of an iridium or ruthenium complex chelated by bipyridine or phenylpyridine ligands (such as $Ru(bipy)_3$ or $Ir(bipy)_3$)[33] (FIG. 1), have similar design constraints to the 'single-step' catalytic chromophores: the complex must absorb a single photon with sufficient energy to drive forward redox reactions. A consequence of this is that photoredox catalysts typically require an absorption maximum at 375–425 nm (REFS[33–35]), which constrains catalyst design by excluding the use of chromophores with lower-energy absorption wavelengths.

Utilizing a Z-scheme, wherein photoredox catalysts become active through multiple photoexcitations at lower-energy wavelengths, presents a strategy to overcome the limitations of monochromophoric catalysts. The utilization of chromophores with lower-energy absorption wavelengths enabled by a Z-scheme would help to overcome the limited penetration depth of high-energy photons typically used in photoredox reactions and prevent competing absorption by substrates and reactants targeted by the catalyst[36]. Z-scheme-based photoredox chemistry could also open new avenues towards multi-electron photoredox reactions. Photosynthesis has optimized such Z-schemes in order to efficiently perform essential multi-electron redox reactions. The most famous example of such a reaction is water oxidation by the Mn_4CaO_5 cluster in photosystem II (PSII), a mechanism that proceeds via consecutive multi-electron redox reactions and stores up to four positive charges, which can then be used in a single concerted catalytic step[3,37,38]. Before discussing bioinspiration in multi-electron reactions, it is important to understand elements one can learn from biology and to consider whether they can be implemented in artificial photoredox catalysts.

An important element of artificial catalysis that differs greatly from biological catalysis is regulation: whereas biology needs to consider regulation of various reactions, which results in modulation of the kinetics for various charge-transfer processes, maximizing the reactivity and turnover frequency of the photoredox catalyst is desired in artificial catalysis. Maximizing the absorption cross section of the chromophores and rates of excitation funnelling to acceptor sites should, therefore, facilitate efficient multi-electron photoredox reactions, such as those involved in cross-coupling chemistry[29,33].

Other important properties that distinguish natural and artificial systems are stability and selectivity. Exposing organisms exhibiting oxygenic photosynthesis to strong light can cause damage to the reaction centre of PSII[39,40]. However, such organisms have developed repair processes whereby biodegradation and protein synthesis can sustain protein turnover with a half-lifetime as low as 30 min (REF.[40]). From an economic or industrial standpoint, such a rapid turnover of artificial catalyst would be too costly; therefore, the chromophores and active sites employed in artificial photocatalysis must be made much more stable than their biological analogues. Also, regarding selectivity, nature often adopts a very different strategy than that employed in artificial systems. An example is CO_2 fixation, where CO_2 is added to a preformed acceptor molecule (ribulose 1,5-bisphosphate) in natural systems, rather than directly activated as in artificial systems. We discuss this further in the section on bioinspired catalyst design.

These distinctions reinforce our earlier statement that bioinspiration should aim to replicate biological functions rather than biological structures, because a biomimetic or artificial PSII may be too short-lived and costly to maintain to be considered economically viable as a photocatalyst.

Multi-electron and multi-photon redox. In order to achieve multi-electron reactivity, natural light-harvesting systems typically contain a large network of electronically coupled pigment–protein complexes, which absorb incident light and funnel photoexcitations to reaction centres, enabling the accumulation of multiple charges. This antennae effect and long-range energy transfer are discussed in more detail in the section on light harvesting; here, we discuss their bioinspired implementation in photocatalysis.

The antennae effect has been used to achieve multi-electron reactivity in bioinspired quantum dot (QD) assemblies[41] (FIG. 1c). By arranging electrostatically bound assemblies of colloidal CdSe QDs, energy-funnelling-enhanced photoredox catalysis of the multi-electron H_2 evolution ($2H^+ + 2e^- \rightarrow H_2$) was demonstrated. As in natural light-harvesting assemblies, excitons are funnelled by Förster-type energy transfer from the majority sensitizer QDs to the minority catalyst QDs, in direct analogy to the 'sensitizer' antennae complexes that surround reaction centres in photosynthesis. QDs have been used with great success in other antennae–photocatalyst systems, such as in a recent demonstration of intermolecular [2+2] cycloadditions with up to 98% switchable regioselectivity and diastereoselectivity[42]. In nature, enzymatic catalysis often exhibits very high selectivity afforded by fine-tuning of intermolecular interactions between substrates and amino acids of the protein scaffold. The exceptional selectivity of this QD photocatalyst was achieved by prearranging the substrates on the QD surface, mimicking natural protein scaffolds, and by tuning the size of the QD to align its triplet energy levels with those of the substrate acceptor molecules, achieving selective triplet energy transfer. QDs and their assemblies are, therefore, systems in which bioinspired design principles can be used to enable highly selective multi-electron reactivity.

Other supramolecular systems that can utilize antennae-assisted multi-electron reactivity are metal–organic frameworks (MOFs). MOFs are supramolecular, periodic and porous architectures consisting of inorganic and organic units linked by strong bonds. Because of the highly variable and controllable combination of inorganic (catalytic) and organic (chromophoric, funnelling) moieties, MOFs are an ideal platform to employ bioinspired concepts for photochemistry. A few examples demonstrated the effectiveness of this strategy. In one case, visible-light-absorbing dyes were used to sensitize MOFs of UiO-66 octahedrons to enable photocatalytic hydrogen production[43]. Another example used a self-assembled, supramolecular MOF combining hexaarmed $[Ru(bipy)_3]$ inorganic and cucurbit[8]uril organic components. When this complex was irradiated with visible light (500 nm), fast multi-electron injection from photosensitive $[Ru(bipy)_3]^{2+}$ to nearby redox-active units was observed, enabling efficient hydrogen production[44].

On smaller scales (not supramolecular), accumulating multiple photoexcited electrons on a common acceptor site has been demonstrated using a molecular pentad[45] (FIG. 1d). Photoexcited electrons in the $Ru(bipy)_3$ complexes undergo rapid charge transfer to a central anthraquinone, while the terminal triarylamine groups become oxidized after donating electrons to $Ru(bipy)_3$. This results in charge-separated states with two holes localized on the peripheral triarylamine groups (one hole on each) and two electrons on the central anthraquinone. Unlike many prior attempts to accumulate multiple carriers onto a single site, which resulted in charge-separated states with lifetimes of, at most, 5 ns, this molecular pentad could sustain charge separation for up to 870 ns. Under acidic conditions, the doubly reduced anthraquinone could be converted into a hydroquinone following intermolecular proton transfer from acidic moieties in the solvent. The hydroquinone photoproduct does not decay through multiple individual steps but, rather, through a concerted proton–electron transfer (CPET) oxidation[46]. The overall lifetime of the CPET-stabilized photoproduct is ~5 µs, approaching the lifetimes of stabilized photoproducts in photosynthetic reaction centres[47].

An example of a system using multiple photons to drive photoredox chemistry was recently demonstrated, wherein a suite of conventional photoredox reactions was performed using near-infrared (NIR) photoexcitation rather than visible or ultraviolet light[36]. This was achieved through a combination of molecules known as triplet sensitizers and annihilators, examples of which are shown in FIG. 1e. The sensitizers can absorb NIR (>700 nm) photons and also convert photogenerated singlet excitons into triplets. These triplet excitons undergo triplet energy transfer to the annihilator chromophores to facilitate triplet–triplet annihilation, an upconversion mechanism by which two triplet excitons are combined to form a singlet exciton with an energy that can potentially be as large as twice the energy of the individual triplets. In this way, NIR (~700 nm) to blue (~500 nm) upconversion is achieved, facilitating photoredox hydrohalogenation, oxidation, cyclization and polymerization reactions with appreciable yields. The authors also calculated that the NIR light penetrated ~304 times deeper than blue light into the reaction solution, harnessing another advantage of utilizing multiple lower-energy photons. Although these reactions do not occur via multi-electron redox steps, multiple electrons and holes must still coordinate to generate the high-energy singlet exciton from the triplet exciton pairs.

These works provide examples of the numerous bioinspired processes that can be tuned to optimize multi-photon-driven photoredox reactions, such as using Z-schemes to improve light absorption in photocatalysts; directing energy and carrier flow to reactive sites; and utilizing proton-coupled electron transfer to extend lifetimes of multiple redox equivalents. The use of triplet annihilators and sensitizers goes beyond biology as an example of an artificial system capable of multi-photon, light-driven catalysis. Such multi-electron (or multi-exciton) concepts may also play an important role in next-generation organic solar cells and photodetectors, in which singlet fission — the reverse process of triplet–triplet annihilation — may be used to improve quantum efficiency[48,49]. Drawing inspiration from biology's ability to precisely manipulate multiple charge carriers simultaneously will benefit the fields of both photocatalysis and photovoltaics.

Bioinspired catalyst design

Artificial solar-energy storage also draws inspiration from biology. Photovoltaic–electrolysis systems can physically separate light absorption and chemical conversion, whereas photoelectrochemical systems combine both processes in one local reaction region[50,51]. Both types of systems require inorganic materials with sophisticated functionality to perform the necessary chemical steps.

In biology, carbon-dioxide conversion has been developed through sophisticated mechanisms to fix CO_2 to sustain the growth of bioorganisms. The success of natural enzymes has inspired research efforts to emulate their structural features in a synthetic analogue to combine the benefits of the biological design with those of synthetic materials. Such model enzymes include carbon monoxide dehydrogenase (CODH) and formate dehydrogenase (FDH), which convert CO_2 to CO and formate, respectively, and nitrogenase, which can reduce N_2 to ammonia. The catalytic reaction happens at a mononuclear or bimetallic transition-metal catalytic centre, but the protein environment around the cofactor is the key to an enzyme's high activity and specificity. The first and second coordination spheres are defined, respectively, as the functional groups bound directly to the metal centre and those that interact with intermediates during reaction but are not directly attached to the redox centre itself. The outer coordination sphere, not directly bound to or interacting with the metal centre, plays the important role of orienting reaction intermediates, shuttling reactants and removing products to maximize efficiency and product selectivity. These structural features together contribute to the high energy efficiency and selectivity of the enzymatic catalysts.

The structure and mechanistic steps of CODH, FDH and nitrogenase have attracted intense research interest in recent years[52–56]. We highlight here two important effects from enzymatic catalysis, the confinement effect and the second-sphere effect (FIG. 2), and draw parallels with inorganic and synthetic catalysts to showcase how the materials chemistry community can learn from biology.

Confinement effects. In NiFe CODH, the CO_2 substrate binds to the Ni redox centre via the C atom, the Fe atom stabilizes one of the O atoms in CO_2 and the second O atom is hydrogen-bonded to the histidine in the second coordination sphere. During the catalytic cycle, the intermediate steps are energetically matched and in equilibrium, thus, the reaction proceeds with a minimal overpotential[57,58]. In contrast to heterogeneous reactions, such as the CO_2 electroreduction reaction (CO_2RR), the substrate confinement orients the reactant with respect to the catalytic centre, stabilizes the molecule in its transition-state geometry and, ultimately, results in a high selectivity towards a single product.

Thus, the spatial control of the reactive intermediates at the active site represents an important focus for catalyst design. Such a spatial control was achieved, for example, in a covalent organic framework (COF) incorporating catalytic cobalt-porphyrin building units (FIG. 2c), in which the COF's structure enabled CO_2 gas adsorption in close proximity to the cobalt porphyrin complex[59]. The precise manipulation of the COF's spatial structure gives an enhanced faradaic efficiency — the percentage of electrons that go towards the desirable product — of above 90% and a turnover number 26 times higher than that of the cobalt porphyrin alone (FIG. 2d). Similarly, an MOF decorated with imidazole units can catalyze methane oxidation to methanol with high selectivity[60]. The ligand and MOF design were judiciously selected to construct an active site inspired by the architecture of methane monooxygenase. The combination of a molecular catalyst and a porous support is an important example of bringing spatial control to synthetic catalysts to maximize the selectivity in the CO_2RR. The active site of the bifunctional catalysts may reconstruct over time; thus, it is important to probe the local environment with operando characterization techniques[61].

Going beyond the molecular scale, confinement effects are also possible by creating structural features on a heterogeneous catalyst to physically control the transport of reactants and intermediates, and, ultimately, steer the reaction outcomes through design. Inversed opal Au and Ag electrodes have been shown to create a confined diffusion gradient of protons that suppresses hydrogen evolution in the CO_2RR[62,63]. The meso-structured catalyst shows a 99% faradaic efficiency, whereas the planar electrode only has ~50% faradaic efficiency. FIGURE 2e shows a nanocavity Cu catalyst that introduces physical confinement of reaction intermediates inside the catalyst's cavity[64]. Different materials geometries lead to different concentration retention of the intermediates on the catalyst's surface and shift the selectivity of the CO-reduction reaction from C2 to C3 products (FIG. 2f). Both examples highlight the importance of geometrical materials design to control the reaction intermediates to tune the product selectivity and reaction paths.

Second-sphere effects. Besides the confinement of substrates, the second coordination sphere also has a variety of important features that have attracted the attention of chemists. Naturally, molecular catalysts have taken advantage of the hydrogen bonding and ion-pair interactions of the ligands to the metal centre in the hope of recreating the efficiency of an enzymatic catalyst[65–67]. Studies on molecular nitrogen-reduction catalysts have shown that the pincer ligands on a Fe complex have an electronic effect that stabilizes the nitrogen binding[68,69]. In CO_2RR molecular catalysts, a common strategy is to incorporate local proton sources via a pendant O–H or N–H moiety in the second coordination sphere of the metal centre[70,71], where the increased local proton concentration can lead to a very high turnover number and a low overpotential. In addition to simply being a proton source, it has also been suggested that the pendant proton donors can provide hydrogen bonding to the O atom of the CO_2 intermediate and improve the reaction selectivity[72–74] (FIG. 2a). The catalytic current density of CO_2RR was shown to be highly dependent on the positional effects of hydrogen bonding for an iron tetraphenylporphyrin system (FIG. 2b). Besides hydrogen bonding, electrostatic interactions from the ligand scaffold have also been utilized to boost the stabilization of the CO_2 adduct in a Fe porphyrin catalyst[75]. Overall,

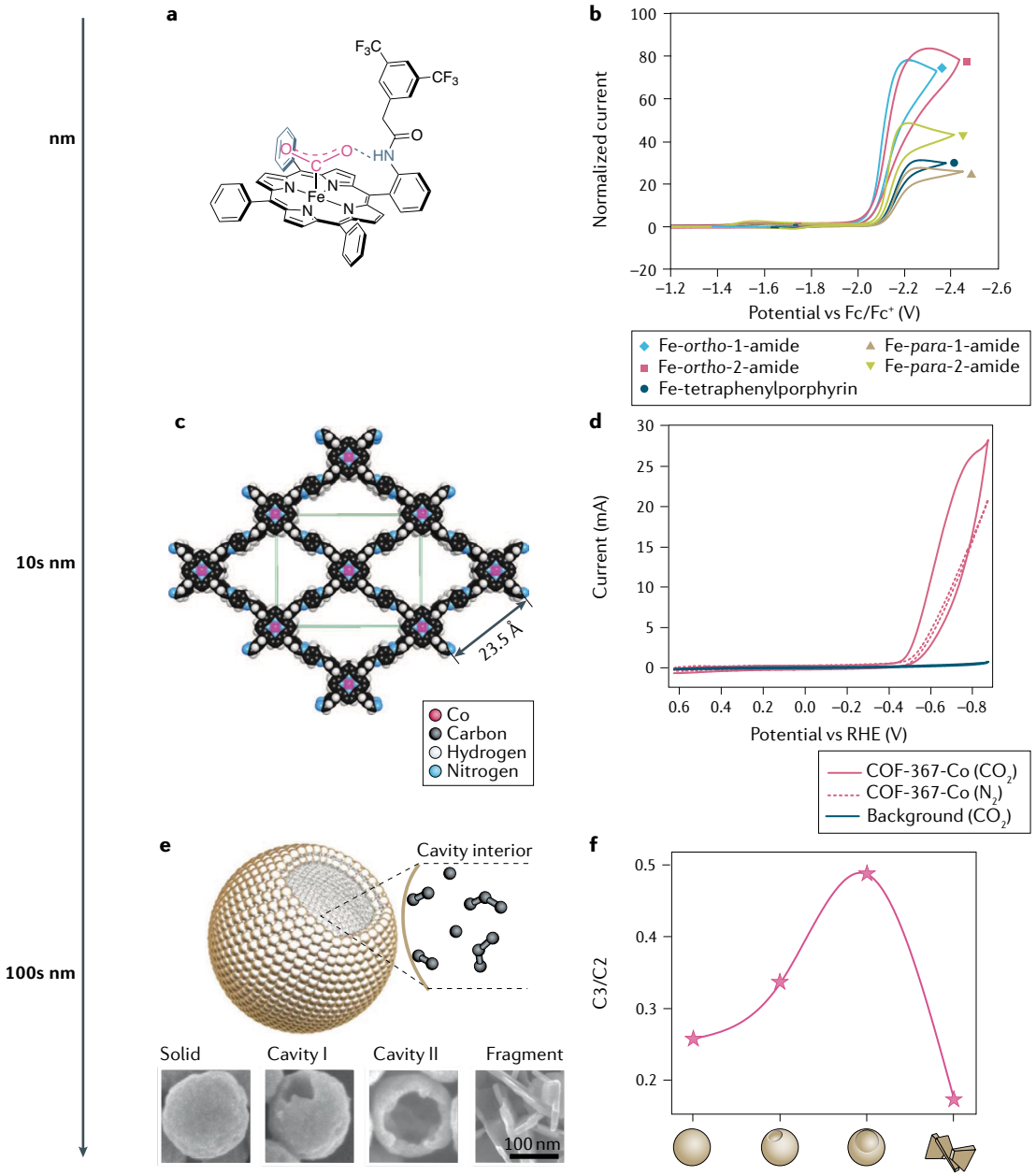

Fig. 2 | **Bio-inspired catalysis at different length scales. a** | Iron tetraphenylporphyrin molecular catalyst with pendant amide groups that can have different positions in the second coordination sphere of the metal core[74]. **b** | Current versus potential curves for the amide-functionalized iron porphyrin catalysts shown in panel **a**, demonstrating the positional effects of the hydrogen bonding on the current density in the CO_2 electroreduction reaction. **c** | A covalent organic framework (COF) incorporating a cobalt molecular catalyst. **d** | Current versus potential curves of the Co-COF catalysts with different pore sizes in a CO_2 (solid lines) and N_2 (dashed lines) electrolyte, demonstrating the confinement effect of intermediates in the CO_2 electroreduction reaction[59]. **e** | Cu catalysts with nanocavities of different opening sizes can trap CO electroreduction-reaction intermediates and increase their retention time. **f** | Faradaic efficiency for Cu nanocavity catalysts with different opening sizes and geometries. C3 products increase for a larger opening due to the geometrical confinement of the reaction intermediates. RHE, reversible hydrogen electrode. Panels **a** and **b** adapted with permission from REF.[74], RSC. Panels **c** and **d** are adapted with permission from REF.[59], AAAS. Panels **e** and **f** are adapted from REF.[64], Springer Nature Limited.

ligand chemistry in the second coordination sphere provides a wealth of research opportunities to translate enzymatic features into synthetic catalysts.

For heterogeneous catalysts, the second-coordination-sphere effects are more challenging to replicate due to the extended nature of the metallic crystal lattice. However, other means to control the local environment of the catalytic active sites have been proposed. Modifications, with molecular additives or carbon-based materials, of a Cu catalyst influence the selectivity of CO_2RR towards longer-chain hydrocarbon products[76,77]. Nanostructured Au and Zn electrodes with high curvature produce a

large local electric field at the tip of the structure, which increases the local concentration gradient of alkali cations and improves the CO_2RR selectivity[78,79]. Although directly mimicking enzyme flexibility is difficult, these examples show that rationally controlling the surface and structure of a synthetic catalyst via innovative designs can lead to enhanced catalytic performance, partly mirroring the benefits offered by the enzyme coordination sphere.

Outer sphere and beyond. Beyond the second sphere, the outer coordination sphere plays a complementary role in controlling the catalytic process. In both nitrogenase and hydrogenase, there are Fe_4S_4 metal clusters with finely tuned redox potentials that facilitate the electron transfer between protein subunits[52,53]. These complex molecular machineries deliver the reactants and electrons precisely to the respective active centres and remove the products to prevent build-up. Such long-range and sophisticated transport over the size of a protein has yet to be implemented in a synthetic catalyst. If obtained, a synthetic analogue could display unprecedentedly high activity and selectivity.

Reactant transport. Going beyond the catalytic centre, management of reactants and products is another important aspect. One of the best known inspirations in biology is the transport of protons and electrons in and across the thylakoid membrane, which maintains a proton gradient, to power photosynthesis. Transport of protons, electrons and products in an artificial CO_2-conversion system presents new engineering opportunities beyond the second coordination sphere of the catalytic active sites.

Understanding the detailed mechanisms of CPET reactions, which are frequently involved in both biological and electrochemical energy-conversion processes[80,81], is essential. In CPET, electrons and protons move in a concerted fashion, avoiding high-energy intermediates that are found in stepwise proton-transfer or electron-transfer steps. One such example is the CO_2-activation step during CO_2RR. Stepwise electron/proton transfer at typical heterogeneous electrocatalysts generates a $*CO_2^-$ anion at high overpotential (−1.9 versus the reversible hydrogen electrode)[82]. By contrast, CPET activation of CO_2 by CODH also leads to a one-electron intermediate, but at a much lower overpotential[83].

Interfacial models of CPET have been reported in recent years in a number of studies to guide the design of heterogeneous catalysts[84,85]. A graphite-conjugated heterogeneous-catalyst system with varying acid–base functional groups that provide surface sites with an acid-dissociation constant, pK_a, a quantitative measure of acidic strength, analogous to that of molecular catalytic systems to control the proton-transfer events, is shown in FIG. 3a. The thermochemistry of the heterogeneous electrocatalytic reactions can be tuned by changing the pK_a of the surface acidic sites and the work function of the electrode material. Thus, electrode materials that are properly designed for concerted proton and electron transfer may ultimately enable us to drive multi-electron and multi-proton reactions at low overpotentials resembling those enabled by biological catalysts.

A common electron-management strategy in bioelectrochemical systems is mediated transport. Mediated systems offer the benefits of a wide range of operating potentials and of a rate of electron transfer that can be controlled by optimizing the interaction between the mediator and the electrode. Mediated electron-transfer systems also allow for decoupling of the oxidative and reductive protein active centres and provide easier access to the buried active sites[86,87]. An example of such a biofuel cell that can convert nitrogen to ammonia under ambient conditions is shown in FIG. 3b. FeMo nitrogenase was used as the biocathode, hydrogenase as the bioanode and methyl viologen as the electron carrier. The system generates a 228-mV open-circuit potential and can convert nitrogen into ammonia: by passing a charge of 60 mC through the fuel cell, 286 nmol of NH_3 were produced per mg of FeMo protein[87]. Other redox-mediated systems have also been successfully demonstrated in biosensors, energy-conversion and energy-storage systems, and electrosynthesis[88].

In an electrochemical system, reactants management is particularly important for the long-term stability of the catalytic process. In CO_2RR, the pH balance, product crossover and accumulation of ions due to electrodialysis can cause failure during prolonged operation. A bipolar membrane (BPM), which generates and directs protons and hydroxide ions to the cathode and anode, respectively, has been demonstrated to manage system stability in CO_2 electrolysis[89,90]. Because protons and hydroxide ions are consumed in the reduction and oxidation reactions, the pH of both anolyte and catholyte can change over time, causing system failure. A BPM can maintain a steady pH and prevent product crossover because of the outward flux of H^+ and OH^- ions. As shown in FIG. 3c, the BPM electrolyzer is more stable than a Nafion-based electrolyzer.

Light harvesting

Energy transfer through photosynthetic membranes. Ubiquitous in photosynthetic light harvesting are antenna complexes that possess large absorption cross sections and exhibit rapid energy transfer across large distances to efficiently funnel photoexcitations into reaction centres, wherein excitons undergo charge separation and energetic electrons can be used to perform useful work. FIGURE 4a shows an image of such a network of exciton-transporting proteins found in purple bacteria such as *Rhodospirillum photometricum*. This network is comprised of two protein complexes, light-harvesting complex 1 (LH1) and LH2) (FIG. 4b). These complexes contain the pigment molecules bacteriochlorophyll (BChl) *a*. Delocalization of the excited states of BChl pigments in LH1 and LH2 gives rise to molecular excitations with redshifted absorption at 800 and 850 nm in the so-called B800 and B850 rings of LH2, and to 875 nm in the B875 ring of LH1. Due to the lower energy of the exciton states in LH1, energy transfer into LH1 is favoured and, so, photoexcitations migrating within the membrane are funnelled into the reaction centres.

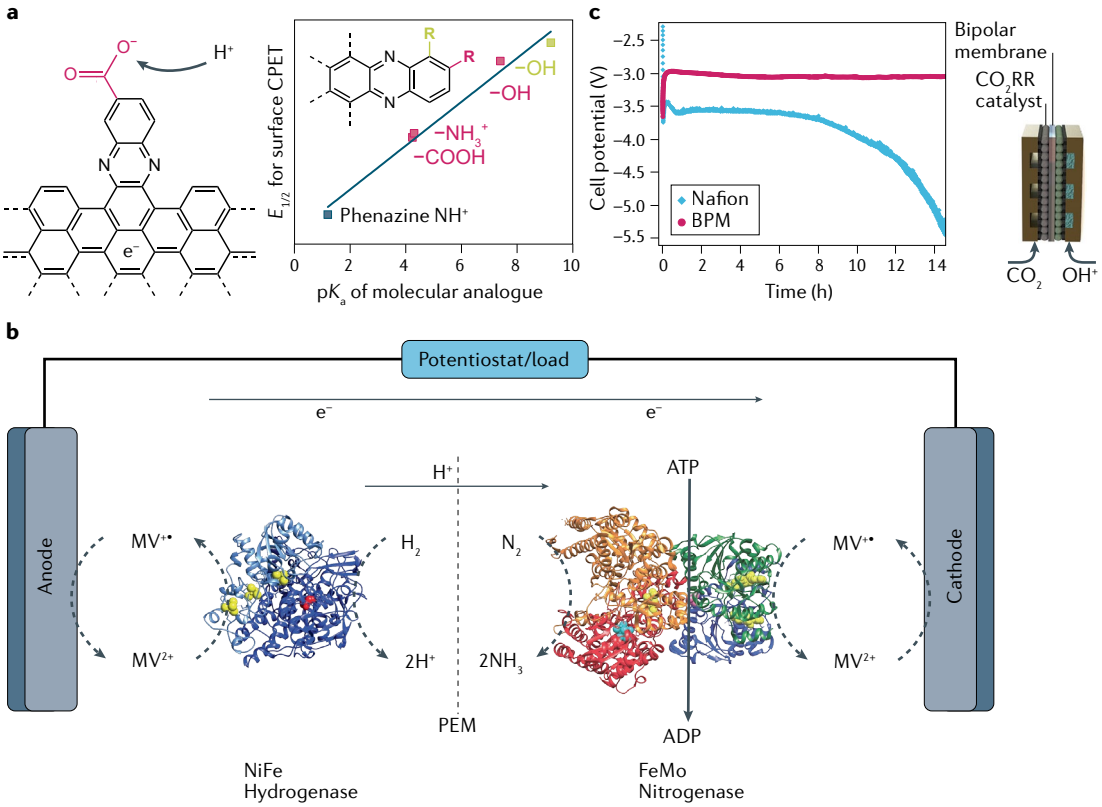

Fig. 3 | **Reactant-transport strategies in catalyst systems. a** | A graphite-conjugated catalyst system with different acid–base functional groups that modify the surface sites. The acid-dissociation constant, pK_a, is determined by the molecular analogue under consideration. The reduction potentials correlate linearly with the pK_a of the molecular analogue (right), demonstrating proton-transport control[84]. **b** | A bioelectrochemical system that demonstrates mediated electron transfer for the generation of NH_3 in an enzymatic fuel cell. Hydrogenase (left) and nitrogenase (right) proteins were used as the anode and cathode catalysts, respectively, to generate hydrogen and ammonia. Methyl viologen (MV) was used as the electron carrier to shuttle electrons between the electrodes and enzymes. **c** | A CO_2 electrolyzer with a bipolar membrane (BPM) as the separation membrane can be used to control and direct the transport of protons and hydroxide ions for electrolysis. The system was more stable when using the BPM rather than a Nafion membrane, which was attributed to the proper control of reactants to balance pH over extended operating times[89]. CO_2RR, CO_2 electroreduction reaction; CPET, concerted proton–electron transfer; $E_{1/2}$, half-wave potential; PEM, proton-exchange membrane. Panel **a** adapted with permission from REF.[84], ACS. Panel **b** adapted with permission from REF.[87], Wiley. Panel **c** adapted with permission from REF.[89], ACS.

Exciton–exciton annihilation experiments have measured exciton diffusion in purple bacteria membranes to occur within a few picoseconds for inter-LH2 hopping and found that the distance travelled by the excitations within the membrane was limited by the size of the system, which was roughly 500–1,000 BChl *a* molecules[91–93]. Similarly long (system-size-limited) exciton-diffusion lengths were also observed in plant membranes[94] and were measured to be up to 2 µm in spinach chloroplasts[95].

The extraordinary singlet-exciton-diffusion lengths found in nature have been replicated in artificial supramolecular complexes: H-aggregated nanofibres composed of a carbonyl-bridged triarylamine core and 4-(5-hexyl-2,2′-bithiophene)-naphthalimide periphery (FIG. 4c) exhibit strikingly long singlet-exciton-diffusion lengths of more than 4 µm across a single structure[96]. These self-assembled structures arrange the carbonyl-bridged triarylamine units co-facially with very small interlayer distances, giving rise to strong electronic coupling on the order of 350 cm^{-1} — similar to the electronic coupling between BChl units in the B850 ring of LH2 (~375 cm^{-1}) — which gives rise to ultrafast energy transfer[97]. J-aggregated nanotubes of amphiphilic cyanine dyes with exciton-transport lengths of 1.6 µm were also reported[98]. Compared with the H-aggregate nanotubes, which have long excited-state lifetimes due to symmetry-forbidden radiative channels, these J-aggregate structures have much shorter lifetimes, yet, exhibit similar diffusion lengths. This means that the diffusion constant must be substantially larger, despite the already large electronic coupling in the H-aggregate system. Importantly, the exciton diffusion in both the H-aggregate and J-aggregate systems was measured at room temperature and, therefore, subject to a similarly noisy environment as in photosynthetic membranes. The efficiency of funnelling can be gauged by the ratio of donor (absorbing) to acceptor (emitting) molecules in an assembly: a higher ratio indicates that excitations travel further within the donor matrix to reach

an emissive acceptor, which indicates a longer diffusion length. Antennae-induced emission with exceptionally high donor:acceptor ratios of 1,500:1 have been demonstrated using non-covalent supramolecular assemblies of oligo(phenylenevinylene), sulfato-β-cyclodextrin and nile red[99]. This donor:acceptor ratio far exceeds the 200 chromophores per reaction centre found in photosynthetic membranes[100].

Although the systems discussed above have not been used directly to enhance photocatalysis (as was the case for the QD assemblies and MOFs discussed earlier), future works integrating these highly efficient antennae complexes and catalysts hold tremendous potential. These examples demonstrate the great progress that has been made in artificial systems, which may now have better exciton-diffusion lengths and donor:acceptor ratios than those found in nature's highly optimized photosynthetic machinery.

Exciton diffusion in OPV active layers. Exciton-diffusion lengths measured in thin films of molecules and polymers used in the active layers of OPVs are typically on the order of 5–10 nm[9,11,101,102]. To contribute to photocurrent in OPVs, excitons must diffuse to a donor–acceptor interface to dissociate into free carriers that then migrate to the electrodes, limiting the thickness of planar OPV active layers and resulting in insufficient optical absorption.

This limitation is overcome in BHJ device architectures, in which mixtures of donor and acceptor molecules are blended throughout the entire active layer.

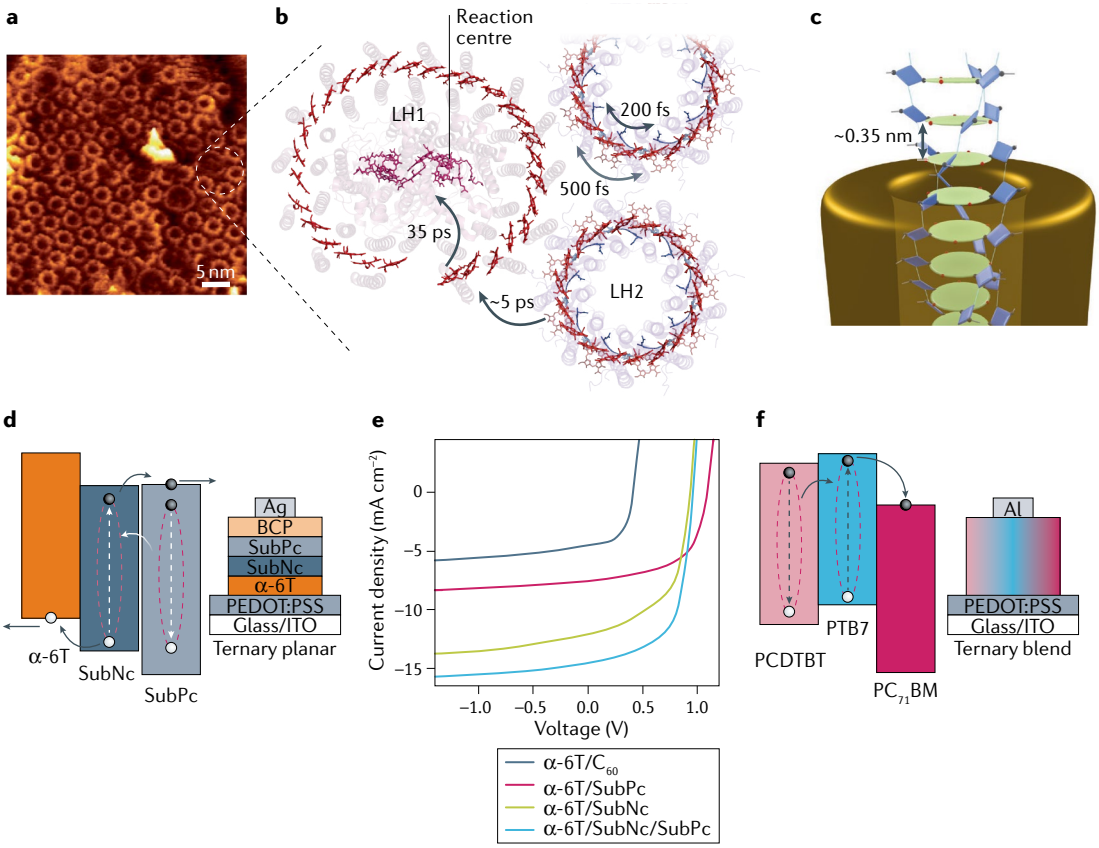

Fig. 4 | **Long-range exciton transport and energy funnelling in photosynthesis and planar, organic, photovoltaic-device architectures. a** | Atomic force microscopy image of the photosynthetic antennae membrane of *Rhodospirillum photometricum*[158,159]. **b** | Molecular structure of the light-harvesting complex 1 (LH1) and LH2 units with associated exciton-transfer timescales within and between the two proteins[93,160,161]. **c** | Self-assembled H-aggregate nanotube comprised of carbonyl-bridged triarylamine core units (green) and 4-(5-hexyl-2,2′-bithiophene)-naphthalimide periphery units (blue). **d** | Trilayer of organic molecules in a ternary planar organic photovoltaic device that exploits long-range energy transfer (white arrow) to increase exciton diffusion lengths, facilitating highly efficient all-planar devices. Black arrows indicate migration of free charge carriers. **e** | Current–voltage characteristics for bilayer and trilayer planar devices, showing an increased photocurrent in the trilayer devices. **f** | Ternary blend of the polymers poly[N-9′-heptadecanyl-2,7-carbazole-alt-5,5-(4′,7′-di-2-thienyl-2′,1′,3′-benzothiadiazole)] (PCDTBT) and polythieno[3,4-b]-thiophene-co-benzodithiophene (PTB7) and fullerene acceptor [6,6]-phenyl C71 butyric acid methyl ester ($PC_{71}BM$)[109]. The insertion of the optically resonant donor polymer PTB7 enables ultrafast Förster resonance energy transfer from PCDTBT, increasing the photocurrent and the overall power-conversion efficiency. α-6T, α-sexithiophene; BCP, bathocuproine; ITO, indium tin oxide; PEDOT, poly(3,4-ethylenedioxythiophene); PSS, poly(styrenesulfonate); SubNc, boron subnaphthalocyanine chloride; SubPc, boron subphthalocyanine chloride. Panel **a** adapted with permission from REF.[158], AAAS. Panel **c** adapted from REF.[96], Springer Nature Limited. Panels **d** and **e** adapted from REF.[108], Springer Nature Limited. Panel **f** adapted with permission from REF.[109], Wiley.

The resulting interpenetrating network has a much higher density of donor–acceptor interfaces, greatly decreasing the distance excitons must travel to reach an interface. Organic solar cells with the highest power-conversion efficiencies almost exclusively use BHJ architectures. Such devices have recently reached impressive efficiencies of 17%[103]. Although organic blends are too complex to serve directly as a testing ground for bioinspired concepts, we can look to developments in planar OPVs, which are better suited to test bioinspired ideas in operating devices. We also discuss how fundamental knowledge gained from such model systems can be translated into higher-order and more efficient blended, organic devices.

The primary mechanism by which singlet excitons transfer between organic molecules in OPV active layers is Förster resonance energy transfer (FRET), which occurs when the transition dipole moments of neighbouring chromophores are dipole–dipole coupled, allowing de-excitation of the donor to create an excitation in the acceptor[104]. Due to energy conservation, these excitations must have the same energy and, so, one main factor that influences the rate of FRET is the spectral overlap of donor emission and acceptor absorbance[105–107]. This is why LH1s have a slightly red-shifted exciton peak (875 nm) relative to LH2's (850 nm): better spectral overlap of LH2 with LH1, rather than LH2 with another LH2, guides excitations into these complexes to be charge separated.

An example of a planar OPV device whose function was improved by enabling such long-range FRET[108] is shown in FIG. 4d. The active layers of the planar OPVs consisted of an α-sexithiophene (α-6T) donor and either one or two acceptor layers, boron subphthalocyanine chloride (SubPc) and boron subnaphthalocyanine chloride (SubNc). SubNc, when incorporated between the α-6T donor and SubPc acceptor, improves the absorption range of the active layer due to its smaller bandgap, but also acts as an electron acceptor from α-6T and as an exciton acceptor from both α-6T and SubPc. The result is an increase in the photocurrent for the trilayer devices without any open-circuit voltage (V_{OC}) loss relative to the bilayer devices (evidenced by the current–voltage characteristics shown in FIG. 4e). The authors found that exciton quenching of SubPc by SubNc occurred at distances as large as 35 nm and concluded that a two-step energy-transfer mechanism is at play, whereby excitons generated in the SubPc layer undergo efficient long-range energy transfer into the SubNc layer, followed by dissociation at the α-6T/SubNc interface.

The same mechanism that drives excitons to reaction centres in photosynthetic membranes is found in the trilayer OPV device: excitons in SubPc have favourable spectral overlap with SubNc and, so, their probability to undergo FRET into the intermediate SubNc layer is greatly improved. This exciton-cascading device architecture thereby extends the diffusion length of excitons along the dimension of the device stack, addressing one of the principal limitations of organic active layers as light harvesters. Extending this concept from planar to blended organic thin films, the utilization of a third organic component in BHJs offers the same benefits. Using an optically resonant donor polymer in a ternary blend increases the photocurrent by widening the absorption range and enabling ultrafast polymer–polymer FRET, forming an exciton relay that can more efficiently transport photogenerated excitations[109] (FIG. 4f). Multi-component FRET cascades have been used in many works to rationalize performance enhancements of ternary[110–112] and quaternary[113] blends over two-component analogues. This energy-funnelling concept has also been applied successfully to other photovoltaic systems, including lead(II) sulfide QDs[114], organic/QD hybrids[115] and low-dimensional perovskites[116–118]. These examples show that concepts rigorously tested in planar OPVs are translatable to blends, indicating that mechanisms similar to those found in biological systems may be at play in some of the most efficient organic devices.

Reducing recombination across interfaces. Energy gradients are utilized by biology in PSII of higher plants and reaction centres of purple bacteria to further stabilize the radical pairs at each step and extend carrier lifetimes through consecutive electron-transfer events[47]. The very rapid initial separation of the radical pair, and the subsequent longer electron-transfer events that further stabilize the charges, are needed to prevent back reactions that would result in recombination and, thus, loss of all the energy contained in the initial photoexcitation.

In OPV, the analogue to the radical pair formed in the first step of the PSII electron gradient are electron–hole pairs in polaronic charge-transfer states at the donor–acceptor interfaces. Recombination of these polaronic electron–hole pairs is detrimental to efficiency, because it can severely limit V_{OC} (REF.[119]). Bioinspired gradual energetic separation of the electron–hole pair should, thus, diminish the effects of back reactions and recover V_{OC}.

This principle has been applied in cascade OPVs that use active layers with built-in energy gradients for excitons, minimizing nonradiative recombination of electrons and holes across interfaces. A series of tetracene molecules and derivatives with extended conjugation were used to fabricate trilayer devices (diphenyl-tetracene/tetracene/rubrene) that exhibited a V_{OC} increase of 40% (+200 meV) relative to monolayer devices, which was rigorously determined to arise due to a modulation of the molecular electron-transfer kinetics: as in photosynthetic reactions, reduction of the electronic-coupling and free-energy differences at the various donor–acceptor interfaces lowered the recombination rate[120]. In the α-6T/SubNc/SubPc device architecture discussed above, this cascade alignment strategy was expanded by inserting various interlayer molecules at the α-6T/SubNc interface, achieving a 180-meV improvement to V_{OC}, determined to arise solely due to suppressed interlayer nonradiative recombination[121]. Another study combined tetracene, SubPc and C_{60} to achieve enhanced photocurrent and improved V_{OC} in trilayer cascade OPVs by increasing optical bandwidth and reducing recombination at interfaces[122].

Ternary organic solar cells with V_{OC} values higher than those of the parent binary blends have been demonstrated[123–125]. In these systems, the cascade-type energy alignment favours exciton dissociation, and one of the acceptor components of the blend can be seen as an interlayer that helps reduce bimolecular recombination at the various junctions. Ternary OPVs with remarkably high fill factors of 77% have been demonstrated, overcoming the recombination thresholds of conventional binary blends[126]. Taken together, these examples show how certain aspects of the working of organic blends used in state-of-the-art photovoltaic devices are analogous to the operation of the natural photosynthetic machinery.

Future prospects of bioinspiration for OPVs. OPV devices using an excitonic cascading mechanism fulfil two bioinspired principles: extending the diffusion length of excitons via long-range energy transfer between layers and reducing interfacial recombination via energy gradients rather than sharp energy offsets at interfaces. Whether these concepts can ultimately be applied controllably in a BHJ and how interlayers can be installed to reduce recombination across interfaces throughout a random or semi-random blend are still open questions. We believe that, as OPV devices continue to break efficiency records and keep being a top contender for next-generation solar cells thanks to their facile, large-area and inexpensive processing, we should turn to the biological mechanisms that grant photosynthetic light harvesters their remarkable quantum yields and examine how their application in OPVs may serve to guide the design of even more efficient devices, regardless of the nature of the heterojunctions.

This recent progress, however, is still rather based on empirical improvements. Due to the long process of molecule synthesis, device design and deposition, and characterization, progress is slow and requires large efforts in synthetic work. Remedying this would require a major leap in understanding the relations between the electronic properties of an individual molecule and those of the solid state, taking into account the complexities of bulk and planar heterojunctions with their non-trivial interface geometries. To be useful for the further development of photovoltaic systems, new theory and simulation methods must offer high precision in the prediction of energies (ideally below 0.1 eV), and they should deliver information on exciton and charge-carrier transport. Furthermore, they should include the recently reported major effects on the energetics in organic materials of quadrupole moments: in particular at interfaces, these effects cause huge energy shifts[127]. These energy shifts allow a novel approach to tune the energy levels in blends[128], thus, potentially reducing the need for repetitive synthesis work.

Paths forwards using bioinspiration

We have surveyed recent advances in several fields, particularly catalysis, where bioinspired concepts — or concepts that were not strictly bioinspired but are at least reminiscent of an analogous biological mechanism — not only improved the overall efficiency of a process but also led to novel functions and capabilities. In light of the great success but even greater potential of bioinspiration in chemistry and materials science, what can be done next to further drive developments in these research areas? In this section, we highlight what we believe are the critical needs and challenges of the numerous communities — organic and inorganic synthetic chemists, materials scientists and engineers, spectroscopists and theorists, biologists — working on bioinspired or bioanalogous catalysis. The targets we identify, and recommendations for how to achieve them, are summarized in TABLE 1 and FIG. 5, and discussed in more detail below.

Develop efficient, precise and endothermic transformations of complex molecules using photons. Developments in photoredox catalysis in the last decade have changed how chemists regard visible light as an energy source to facilitate the construction of complex molecular architectures, but energetically demanding reactions with extreme selectivity, such as the activation of C–H bonds to form endothermic and valuable products, remain elusive to both the homogeneous and heterogeneous catalysis communities. We posit that photoredox catalysts could conceivably help drive highly endothermic and selective reactions, aided by concepts borrowed from nature.

Efficient photoredox catalysts require large absorption cross sections to generate excited states, high quantum yields of formation of these reactive excited states and long excited-state lifetimes to facilitate diffusion of the catalyst to reactants in solution[129]. These requirements can be addressed by targeting the optical properties of the ligands themselves. One of the major limitations of many metal photoredox catalysts is that they are limited by the amount of light they can absorb, thus, increasing their absorption cross section could yield faster turnover. Conventional metal photocatalysts like $Ru(bipy)_3$ depend on high-energy metal-to-ligand charge-transfer transitions. This transforms the metal centre into an oxidant, and one of three bipy ligands into a reductant. The molar absorptivity of such transitions is on the order of 10,000 $M^{-1}\,cm^{-1}$, and one route to improving the overall absorption of the catalyst could be to employ additional strongly absorbing chromophores attached to the bipy ligands. The concept of an 'antenna' ligand, which could funnel excitations into $Ru(bipy)_3$ photoredox catalysts, is analogous to how biology uses vast antennae networks to absorb more solar light and funnel excitons in reactions.

We discussed how photosynthetic reaction centres make use of an energy gradient to drive charge separation through a series of electron-transfer steps. Though this incurs an energetic penalty, the reactions centres achieve remarkably long-lived electronic excited states with microsecond and millisecond lifetimes, required for multiple redox equivalents to accumulate to enable water splitting. These lifetimes are longer than the excited-state lifetimes of metal photoredox catalysts (with an upper bound of ~6 μs), suggesting that this electron–acceptor strategy used by nature to extend carrier lifetimes could be a rich source of bioinspiration to apply to photoredox catalysis in efforts to improve overall

Table 1 | **Objectives, recommendations and targets for the future of bioinspiration in materials science and chemistry**

Objectives	Recommendations	Specific targets
Devise efficient, precise and endothermic organic transformations: access thermodynamically uphill products with the extreme specificity and selectivity of biology, beyond the capabilities of conventional organic transformations	Utilize bioinspired multi-photon-harvesting Z-schemes and multiple carrier-accumulation strategies to augment conventional photoredox catalysts with multi-electron reactivity	Use chromophoric ligands with large oscillator strengths, strongly coupled to photocatalysts, as excitation-funnelling antennae Exploit broadband absorbing chromophores and catalysts coupled in a Z-scheme to make use of multiple lower-energy photons Use triplet–triplet annihilation to convert near-infrared light into higher-energy photons using molecules and semiconductors Gain control and mechanistic understanding of excited-state dynamics of multi-electron photoredox catalysts
Design effective and specific catalysts: overcome energetic scaling relationships in heterogeneous and homogeneous catalysts, and control transport of reactants and products	Utilize bioinspired second-shell design of catalytic surroundings and maximize efficiencies of individual steps in cascade systems Use multi-component active sites beyond single metals	Design dynamic control of the local environment via ligand chemistry and MOF and COF structures Control product selectivity through reaction intermediates confinement Use cascade system (analogous to enzyme cascades), $CO_2 \rightarrow CO \rightarrow$ octane, or electro-upgrade or bio-upgrade Engineer design for scaled-up heterogeneous electrosynthesis: systems and reactants management (such as H^+, OH^-, e^-, CO_2 and HCO_3^-)
Deepen understanding: quantify and control true atomic compositions and configurations of heterogeneous catalysts; unify improved characterization (spectroscopy and imaging) analysis with new theoretical models supporting advanced catalyst design	Develop better theoretical models and computational methods through feedback with experimental operando tools	Develop more quantitative and broadly applicable theories for understanding and predicting homogeneous and heterogeneous catalytic behaviour Improve operando synchrotron techniques to directly monitor catalytic reactions Use grazing-incidence X-ray absorption spectroscopy to more precisely evaluate surfaces Develop nanoscale and ultrafast time-resolved probes of catalytic-reaction mechanisms
Accelerate materials and catalyst discovery: accelerate the intuitive but slow discovery of catalysts, towards the rapid and high-throughput creation of libraries of materials or molecules	Look to biology to target a chemical space and use a closed loop of machine learning and robotic high-throughput synthesis to optimize synthesis, building on a deepened understanding	Use inverse molecular design to search for target molecules Employ robotic synthesis of catalysts and high-throughput assays of homogeneous and heterogeneous catalytic reactions Use machine learning to guide catalytic design and infer mechanisms that permit high efficiency and selectivity

COF, covalent organic framework; MOF, metal–organic framework.

efficiency, and also to realize catalysts that can perform multi-electron transformations, as in photosynthesis. This could also be achieved by tailoring the ligands binding the metal centre, functionalizing them with good electron-acceptor molecules, such as napthalenediimides or perylenediimides. This would help to fully localize electrons on the ligand, away from the metal centre, reducing the probability of recombination and, thus, extend the overall lifetime of the charges to perform chemistry.

Another promising approach to improve the efficiency of photochemical reactions is strong light–matter coupling. Strong light–matter interactions can be achieved if many emitters are collectively coupled to a single mode, such as in optical cavities, or if the effective volume in the electromagnetic environment is drastically reduced, such as for nanoplasmonic systems. It has been experimentally demonstrated that strong light–matter coupling can effectively change the outcome of chemical reactions without the need for any chemical substitutions[130–132], whereas the first ab initio studies of strongly coupled light–matter systems involved in chemical reactions[133,134] demonstrated that vibrational strong coupling or changes in electron–photon (polaritonic) potential-energy surfaces[135,136] could be used to quench specific chemical pathways. These works highlight that polaritonic effects can effectively influence the chemical landscape and potentially improve photocatalyst efficiency.

Controlling and directing chemical reactions in optical cavities opens many new directions for photochemistry. For example, chemical reactions could be performed in optical cavities without the need to explicitly drive the system. Looking forwards, more accurate ab initio models will guide experimentalists to promising chemical reactions that can be altered under strong–light matter coupling. Controlling the coupling strength in optical cavities has the potential to either directly increase the probability of certain chemical-reaction pathways or quench undesired pathways.

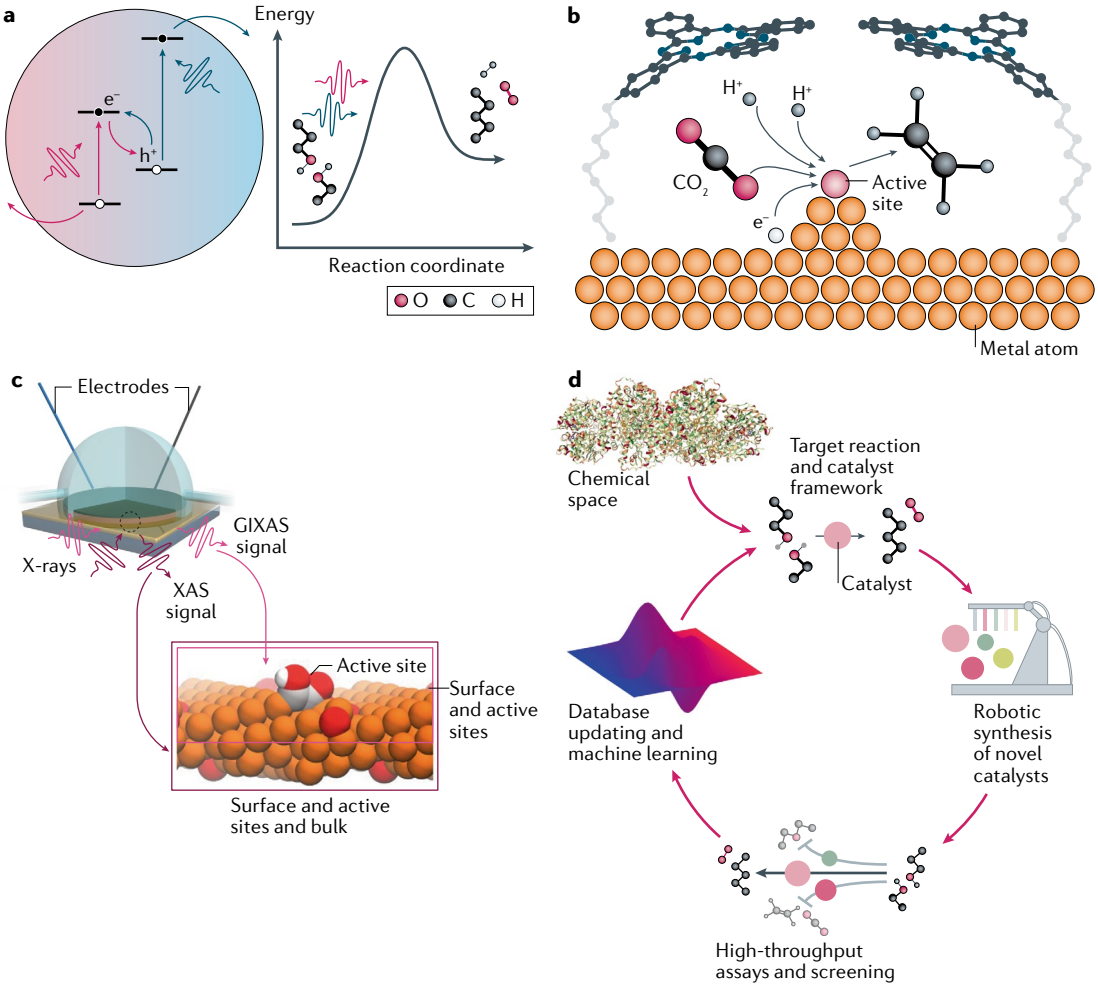

Fig. 5 | **Bioinspiration in materials science and chemistry. a** | A generic Z-scheme photoredox catalyst that can access useful endothermic products via multi-photon photoredox catalysis. By combining two or more chromophores that absorb light strongly at different wavelengths (illustrated by the impinging red and blue photons) and coupling them in a Z-scheme, multiple lower-energy photons can be used to overcome energetic barriers and drive forward endothermic reactions. **b** | Heterogeneous catalytic surfaces suffer from inefficiencies due to short-lived intermediate species that are lost before being fully converted into a desired product. If nanoconfinement and dynamic control (here, imagined using porphyrin molecules tethered to the metal surface) could be used to control transport and coordination of reactant CO_2 molecules, protons and electrons, the transient intermediates formed during the catalytic cycle could be maintained near the active site, and higher carbon products such as ethylene can be formed. **c** | Illustration of an envisioned operando grazing-incidence X-ray absorption spectroscopy (GIXAS) experiment, in which lower incident angles enable probing of surfaces and active sites, and avoid penetration into the bulk of the catalyst (left). One step of a density functional theory model used to simulate the hydrogenation of CO bound to CH_4 (right). In situ or operando spectroscopies performed on catalysts can deepen our understanding of mechanisms and reactivity by directly probing activity, rather than inferring information from pre-reaction and post-reaction measurements. Uniting experiment and theory from operando studies will enable the building of better theoretical models that can be truly and quantitatively predictive, and help guide materials design. **d** | By combining high-throughput synthesis with machine learning, a biologically inspired chemical space can seed a closed loop to accelerate the discovery of novel and optimal catalysts for a given reaction. XAS, X-ray absorption spectroscopy. Panel **c** adapted from REFS[144,162], Springer Nature Limited.

Overall, we believe that accessing new photochemistry is tied to implementing novel functionalities in the ligands of the photocatalyst and rethinking how to exploit light–matter interactions towards chemical reactivity and selectivity. Biology offers inspiring examples of how to achieve longer excited lifetimes, as well as how to accumulate multiple redox equivalents through excitation funnelling. Utilization of these bioinspired concepts in photoredox catalysis — striving to replicate biological function and not structure — could expand the already impressive scope of complex and specific organic reactions that can be performed with the assistance of photons (FIG. 5a).

Hybrid design of catalysts with tailored surface properties. Enzymes present a number of attractive properties that continue to provide important insights for catalyst design. Complementing enzymes' limitations, synthetic heterogeneous catalysts can be prepared in large batches and are less air sensitive than enzymes. From molecular

to heterogeneous catalysts, the bioinspired approach for catalyst design has been successfully demonstrated. However, to advance electrocatalytic technologies further, we identify two goals that need to be achieved: obtaining dynamic control of the catalytic active sites and moving beyond single systems for multi-electron, multi-proton catalytic reactions; that is, utilizing a cascade system.

From a materials-design perspective, one of the most important aspects of biology that we have not been able to mimic is the dynamic response of natural systems. One such example is a self-healing catalyst. Heterogeneous catalysts deactivate over time due to reconstruction or poisoning, which leads to costly replacement. Biology has specific processes for repairing or replacing damaged proteins, nucleic acids, organelles and cells to maintain continuous functionality. Although self-healing catalysts have been demonstrated in some applications[137,138], the implementation of a dynamic response is limited to a narrow range of materials, and a general approach is needed to widen these applications. Another type of dynamic control is the flexibility of the active sites. Although we have showcased several examples of local environmental control via clever materials design, enzymes still have many features that we have not fully replicated: the relaying function of cofactors, the flexible movement of functional groups, which is influenced by the conformational sampling of the environment, the electrostatic fields that facilitate chemistry and the efficient transport of reactants and products. Synthetic catalysts still require major advances to achieve such dynamic control of their active sites (FIG. 5b).

In addition to simple products such as CO and formate, enzymes can be combined to sequentially convert a feedstock such as CO_2 into higher-value chemicals[139,140]. Such cascade reactions are possible for enzymes due to the high conversion efficiency and selectivity of each enzymatic subunit. One example is the sequential reduction of CO_2 to formate and formaldehyde to produce methanol[141]. A material analogue of an enzyme cascade reaction has been reported with interdigitated Au and Cu systems, in which the Au catalyst enhanced the *CO coverage on Cu (REF.[142]), leading to an enhanced generation of oxygenated products. More sophisticated heterogeneous cascade systems have not been reported due to the difficulties in controlling chemical transport and selectivity loss, and in balancing the different production/consumption rates of the individual catalytic subunits. Nevertheless, a synthetic mimic of a cascade reaction could be a promising strategy to achieve the formation of long-chain (C_{3+}) hydrocarbons that have otherwise been unattainable so far.

Overall, combining the efforts of the biology and materials science communities provides an exciting opportunity to design catalysts with record-breaking activity and selectivity towards a wide range of valuable chemical products.

Deepen understanding through advanced spectroscopies and theoretical models. Despite tremendous advances in heterogeneous catalysis to transform inert small molecules such as CO_2, N_2 and H_2O into useful products, and despite models that explain their reactivity, our understanding of these catalysts remains undeniably limited. Similar to enzymes, heterogeneous catalytic surfaces are highly dynamic during operation, meaning that a suite of characterizations pre-reaction and post-reaction can offer some insight into the importance of atomic configurations or morphology, but they cannot guarantee a fully accurate description of the system during operation. This limitation has major consequences for both experimentalists and theorists: the disparity between what we put into experiments and what we put into simulations is the same as the disparity between what we think occurs in an experiment versus what actually happens. This disparity may also prevent us from knowing if bioinspired concepts implemented into artificial materials are functioning as intended. To guide the design of the 'perfect' catalyst, three areas of advancement are required: more precise operando characterization techniques, more quantitative theories for in silico catalyst design and stronger unification of operando experiments and theories using large datasets and machine learning.

On the characterization front, a recurring challenge is the identification and quantification of the catalytic active sites. Current in situ or operando characterization techniques include optical techniques (infrared and Raman spectroscopy, near-field optical microscopy), X-ray-based techniques (X-ray absorption spectroscopy (XAS) and X-ray photoelectron spectroscopy) and electron-based techniques (liquid-phase transmission electron microscopy and scanning probe microscopy)[61,143]. However, the determination of the precise location and distribution of the catalytic sites remains elusive, and many techniques cannot yet be applied operando or during catalysis. Also, not all of the intermediates proposed by computational studies for CO_2RR are observable during characterization, leading to an incomplete picture of the catalytic path. Of central importance to progress in this field is the development of new techniques that will address many of these challenges. X-ray synchrotron techniques have been particularly successful in this area: operando soft or hard XAS has been used on copper-based and iron-based nanostructures to probe CO_2RR catalytic active sites that enable C–C coupling and their alteration with changing potential[144,145]. Limitations of this type of experiment include the necessity of a synchrotron X-ray source and the non-selective probing of the entire catalytic material instead of only the active surface layers. Further developments in operando XAS to probe catalytic reactions could involve non-synchrotron X-ray sources that are sufficiently tunable[146] and bright to enable a more widespread use of this technique, and the use of grazing-incidence XAS to target surfaces that contain active sites instead of the bulk[147] (FIG. 5c). In a step beyond, we would seek to discriminate the portions of surface that are catalytically active, and to collect XAS data specifically for those sites.

In biology, a detailed view of the exceptionally complex water-splitting mechanism in PSII has long been elusive, but tremendous progress has been made using femtosecond X-ray pulses[37,148,149], which allowed for time-resolved crystallography of PSII under

photoexcitation[150]. It is feasible to apply these 'champion experiments' to individual and well-known systems, but it would be a great challenge to apply them to the vast variety of artificial catalytic systems. Translating these techniques to artificial systems would require the establishment of more facilities capable of these measurements or the development of smaller-scale systems that can generate femtosecond X-rays.

Operando XAS experiments can be complemented by density functional theory (DFT) studies. This combination allowed for the correlation of the computationally predicted reaction pathways with the experimentally measured metallic morphology and oxidation state. DFT calculations, corroborated by experimental data, have also been successful in investigating proton-coupled electron transfer in bioinspired catalysts based on CODH (as discussed in the subsection on reactant transport)[151]. These applications exemplify the importance of uniting experimentalists and theorists to advance the field of heterogeneous catalysis. The advancement of characterization techniques, theoretical models and computational methods can guide the in silico design of new catalysts. Current DFT calculations of catalytic bulk solids and surfaces are often based on idealized models of perfect crystal facets or prearranged periodic structures, which are not representative of the real catalytic surface. Moreover, the description of the kinetics of heterogeneous reactions requires advanced computational techniques. For photocatalysis, expensive calculations such as time-dependent DFT are often required to capture excited-state properties.

Areas of improvement on the theoretical front include more accurate structural models based on information from experiments that capture the real catalytic surface as well as the local solvent environment; more comprehensive microkinetic models that account for the kinetic barriers as well as the thermodynamics of all possible reaction pathways; and improved throughput of ground-state and excited-state calculations for electrocatalysis and photocatalysts. For example, machine learning has recently been used to construct accurate density functionals for realistic molecular systems, a promising advance that could be translated to photocatalytic or heterogeneous systems[152]. Continued optimization of the computational models and algorithms can certainly help us to achieve better catalyst designs and overcome the energy challenges. Strengthening the bridge between experiments and theory, large and open-access datasets of operando experiments combined with accurate, high-throughput modelling could be fed into machine-learning algorithms; optimal catalysts could be predicted, tested and characterized experimentally, and then examined in detail to understand the significance of bioinspired concepts to enhance function. Such analyses would help discover general structure–activity relationships. We elaborate on the potential role of bioinspiration in machine-learning-accelerated materials discovery in the next subsection.

Accelerate materials discovery using robotic synthesis and machine learning. Biological systems with essential functions, such as the FeMo cofactor of nitrogenase that catalyzes the conversion of N_2 into NH_3, exist in chemical spaces that offer potential starting points for replicating or improving on these functions in artificial systems. The catalytic capabilities of the FeMo complex have inspired synthetic inorganic chemists to target chemical spaces containing similar elements: sulfur-rich iron complexes that can bind N_2 or molybdenum complexes that can activate N_2. Synthetic complexes aiming to replicate FeMo's function include sulfur-rich iron complexes, which were used to obtain nitrogen fixation in Fe–N_2 complexes[153], and Fe–K complexes used to transform N_2 into NH_3 (REF.[154]).

These results indicate that targeting a given chemical space inspired by nature can indeed lead to artificial systems that exhibit the desired functions. However, these breakthroughs were achieved through experiments that, although intuitive, were inherently slow and exploratory, and, in many cases, not optimized within a local chemical space for the intended application. It would be an arduous task to optimize a system (for example, for better binding of substrate molecules or high turnover frequencies for the catalytic transformation) through mostly unassisted trial-and-error experimentation. This is, in fact, what has been achieved in nature: millions of years of random mutations and evolution allowed enzymes to naturally optimize their 3D structure in order to achieve optimal catalysis. A similar optimization for artificial catalysts on a much shorter timescale could be immensely aided by accelerated materials discovery, by combining machine learning with automated robotic synthesis.

The past few years have seen important developments in the application of machine learning to materials discovery; a prominent example was the demonstration of a methodology combining machine learning, industrial synthetic expertise, quantum chemistry and cheminformatics to design molecules for organic light-emitting diodes with excellent performance[155]. A recent major advance further demonstrated the utility of machine learning for discovering new chemical reactivity through the use of a liquid-handling robot coupled to automatic and real-time reaction analysis with various spectroscopies. Operating in a closed feedback loop in which reaction databases are updated after analysis, a machine-learning algorithm was used to scan the chemical space and set the next experiments controlled by the robot[156]. Predictions generated from this trained model were then used towards the discovery of four new reactions, making this a powerful proof that machine learning, coupled with robotic high-throughput synthesis and analysis, has enormous potential for developing novel catalytic and synthetic organic chemistry. Another recent study used machine learning and ultra-high-throughput screening to predict the performance of C–N cross-coupling reactions; the use of an appropriate model (random forest) led to accurate out-of-sample predictability even with sparse training sets, further demonstrating the promise of machine learning for complex catalytic organic transformations[157].

These examples illustrate how machine learning and robotic synthesis are poised to be transformative to materials discovery. As we have discussed, a deeper

understanding of biological systems gives deeper insight into the chemical spaces nature uses to achieve reactivity coveted by energy scientists. In the same way, expanding our fundamental understanding of what cannot be replicated from biology (for example, complex protein scaffolds) but can inspire systems with similar functionality (for example, nanostructured catalytic environments and active sites) helps to further define a chemical space to navigate. We believe that an important step forwards in the development of bioinspired materials will be to use biology to help choose chemical spaces in which to search to learn how to perform a given reaction with high efficiency and precision, and to use the rapidly developing tools in robotic synthesis and machine learning to implement a closed-loop approach to discover artificial systems that can perform the desired chemistry (FIG. 5d).

Conclusions

By evolving from a wide variety of conditions over a long period of time, biology has created organisms that exhibit remarkable photophysical and catalytic properties. Capturing atmospheric levels of carbon dioxide and rendering them into sugars, turning extremely unreactive nitrogen into ammonia and using water to create oxygen and hydrogen gas are essential processes to cellular life. The resources used by nature are the same resources humankind wishes to tap into more effectively, for example, to turn carbon dioxide into fuels and harvest solar light to generate electricity. By studying proteins such as carbonic-dehydrogenases, PSII and LH2, we can learn how nature engineered them to carry out such remarkable functions, why they work so well and, ultimately, use this knowledge towards bioinspired design principles. These principles need not aim to directly replicate these systems: we have seen that the application of bioinspired principles to totally different classes of materials can sometimes improve or expand functionality. Examples include novel approaches to photoredox catalysis by using two low-energy photons to perform higher-energy redox reactions, analogous to the Z-scheme of PSII, or using a bioinspired nanoconfinement strategy on a rigid and completely inorganic heterogeneous catalyst to confine intermediates and produce higher carbon products.

In the case of enzymes such as nitrogenase and PSII, the exact mechanisms of how nature breaks the triple bond of nitrogen, or simultaneously uses multiple electrons to split water, remain elusive. In addition to trying to scope these systems for bioinspiration for man-made materials, biologists and materials scientists must continue to try to fully understand these processes to ensure that we do not build new paradigms and theories from incorrect assumptions. As increasingly advanced spectroscopies, structurally investigative techniques and theoretical models emerge, we can learn more about these fascinating natural systems. This knowledge will enable us to further extend the application of bioinspiration into engineered materials in order to improve their performance and expand their functionality.

Published online: 07 August 2020

1. Lewis, N. S. & Nocera, D. G. Powering the planet: chemical challenges in solar energy utilization. *Proc. Natl Acad. Sci. USA* **103**, 15729–15735 (2006).
2. Hammarström, L. & Hammes-Schiffer, S. Artificial photosynthesis and solar fuels. *Acc. Chem. Res.* **42**, 1859–1860 (2009).
3. Babcock, G. T. et al. Water oxidation in photosystem II: from radical chemistry to multielectron chemistry. *Biochemistry* **28**, 9557–9565 (1989).
4. Zhu, X.-G., Long, S. P. & Ort, D. R. What is the maximum efficiency with which photosynthesis can convert solar energy into biomass? *Curr. Opin. Biotechnol.* **19**, 153–159 (2008).
5. Tanaka, S. & Marcus, R. A. Electron transfer model for the electric field effect on quantum yield of charge separation in bacterial photosynthetic reaction centers. *J. Phys. Chem. B* **101**, 5031–5045 (1997).
6. Loach, P. A. & Sekura, D. L. Primary photochemistry and electron transport in *Rhodospirillum rubrum*. *Biochemistry* **7**, 2642–2649 (1968).
7. Cho, H. M., Mancino, L. J. & Blankenship, R. E. Light saturation curves and quantum yields in reaction centers from photosynthetic bacteria. *Biophys. J.* **45**, 455–461 (1984).
8. van Grondelle, R., Dekker, J. P., Gillbro, T. & Sundstrom, V. Energy transfer and trapping in photosynthesis. *Biochim. Biophys. Acta* **1187**, 1–65 (1994).
9. Penwell, S. B., Ginsberg, L. D. S., Noriega, R. & Ginsberg, N. S. Resolving ultrafast exciton migration in organic solids at the nanoscale. *Nat. Mater.* **16**, 1136–1141 (2017).
10. Markov, D. E., Amsterdam, E., Blom, P. W. M., Sieval, A. B. & Hummelen, J. C. Accurate measurement of the exciton diffusion length in a conjugated polymer using a heterostructure with a side-chain cross-linked fullerene layer. *J. Phys. Chem. A* **109**, 5266–5274 (2005).
11. Mikhnenko, O. V., Blom, P. W. M. & Nguyen, T.-Q. Exciton diffusion in organic semiconductors. *Energy Environ. Sci.* **8**, 1867–1888 (2015).
12. Bolton, J. R., Strickler, S. J. & Connolly, J. S. Limiting and realizable efficiencies of solar photolysis of water. *Nature* **316**, 495–500 (1985).
13. Kuriki, R. et al. Nature-inspired, highly durable CO_2 reduction system consisting of a binuclear ruthenium(ii) complex and an organic semiconductor using visible light. *J. Am. Chem. Soc.* **138**, 5159–5170 (2016).
14. Khaselev, O. & Turner, J. A. A monolithic photovoltaic-photoelectrochemical device for hydrogen production via water splitting. *Science* **280**, 425–427 (1998).
15. Cheng, W.-H. et al. Monolithic photoelectrochemical device for direct water splitting with 19% efficiency. *ACS Energy Lett.* **3**, 1795–1800 (2018).
16. Jin, J., Yu, J., Guo, D., Cui, C. & Ho, W. A hierarchical Z-scheme CdS–WO_3 photocatalyst with enhanced CO_2 reduction activity. *Small* **11**, 5262–5271 (2015).
17. Jiang, Z. et al. A hierarchical Z-scheme α-Fe_2O_3/g-C_3N_4 hybrid for enhanced photocatalytic CO_2 reduction. *Adv. Mater.* **30**, 1706108 (2018).
18. Di, T., Zhu, B., Cheng, B., Yu, J. & Xu, J. A direct Z-scheme g-C_3N_4/SnS_2 photocatalyst with superior visible-light CO_2 reduction performance. *J. Catal.* **352**, 532–541 (2017).
19. Wang, L., Zheng, X., Chen, L., Xiong, Y. & Xu, H. Van der Waals heterostructures comprised of ultrathin polymer nanosheets for efficient Z-scheme overall water splitting. *Angew. Chem.* **130**, 3512–3516 (2018).
20. Sahara, G. et al. Photoelectrochemical reduction of CO_2 coupled to water oxidation using a photocathode with a Ru(II)–Re(I) complex photocatalyst and a CoO_x/TaON photoanode. *J. Am. Chem. Soc.* **138**, 14152–14158 (2016).
21. Sahara, G. et al. Photoelectrochemical CO_2 reduction using a Ru(ii)–Re(i) multinuclear metal complex on a p-type semiconducting NiO electrode. *Chem. Commun.* **51**, 10722–10725 (2015).
22. Yoshitomi, F., Sekizawa, K., Maeda, K. & Ishitani, O. Selective formic acid production via CO_2 reduction with visible light using a hybrid of a perovskite tantalum oxynitride and a binuclear ruthenium(II) complex. *ACS Appl. Mater. Interfaces* **7**, 13092–13097 (2015).
23. Iwase, A. et al. Water splitting and CO_2 reduction under visible light irradiation using Z-scheme systems consisting of metal sulfides, CoOx-Loaded $BiVO_4$, and a reduced graphene oxide electron mediator. *J. Am. Chem. Soc.* **138**, 10260–10264 (2016).
24. Muraoka, K. et al. A visible-light-driven Z-scheme CO_2 reduction system using Ta_3N_5 and a Ru(II) binuclear complex. *Bull. Chem. Soc. Jpn* **92**, 124–126 (2019).
25. Shaw, M. H., Twilton, J. & MacMillan, D. W. C. Photoredox catalysis in organic chemistry. *J. Org. Chem.* **81**, 6898–6926 (2016).
26. Narayanam, J. M. R. & Stephenson, C. R. J. Visible light photoredox catalysis: applications in organic synthesis. *Chem. Soc. Rev.* **40**, 102–113 (2011).
27. Xuan, J. & Xiao, W.-J. Visible-light photoredox catalysis. *Angew. Chem. Int. Ed.* **51**, 6828–6838 (2012).
28. Reckenthäler, M. & Griesbeck, A. G. Photoredox catalysis for organic syntheses. *Adv. Synth. Catal.* **355**, 2727–2744 (2013).
29. Prier, C. K., Rankic, D. A. & MacMillan, D. W. C. Visible light photoredox catalysis with transition metal complexes: applications in organic synthesis. *Chem. Rev.* **113**, 5322–5363 (2013).
30. Schultz, D. M. & Yoon, T. P. Solar synthesis: prospects in visible light photocatalysis. *Science* **343**, 1239176 (2014).
31. Vila, C. Merging visible-light-photoredox and nickel catalysis. *ChemCatChem* **7**, 1790–1793 (2015).
32. Levin, M. D., Kim, S. & Toste, F. D. Photoredox catalysis unlocks single-electron elementary steps in transition metal catalyzed cross-coupling. *ACS Cent. Sci.* **2**, 293–301 (2016).
33. Twilton, J. et al. The merger of transition metal and photocatalysis. *Nat. Rev. Chem.* **1**, 0052 (2017).
34. Huo, H. et al. Asymmetric photoredox transition-metal catalysis activated by visible light. *Nature* **515**, 100–103 (2014).
35. Iqbal, N., Jung, J., Park, S. & Cho, E. J. Controlled trifluoromethylation reactions of alkynes through visible-light photoredox catalysis. *Angew. Chem.* **126**, 549–552 (2014).
36. Ravetz, B. D. et al. Photoredox catalysis using infrared light via triplet fusion upconversion. *Nature* **565**, 343–346 (2019).

37. Suga, M. et al. Native structure of photosystem II at 1.95 Å resolution viewed by femtosecond X-ray pulses. *Nature* **517**, 99–103 (2015).
38. Najafpour, M. M. et al. Proposed mechanisms for water oxidation by Photosystem II and nanosized manganese oxides. *Biochim. Biophys. Acta* **1858**, 156–174 (2017).
39. Najafpour, M. M. et al. Damage management in water-oxidizing catalysts: from photosystem II to nanosized metal oxides. *ACS Catal.* **5**, 1499–1512 (2015).
40. Aro, E.-M., Virgin, I. & Andersson, B. Photoinhibition of photosystem II. inactivation, protein damage and turnover. *Biochim. Biophys. Acta* **1143**, 113–134 (1993).
41. Kodaimati, M. S., Lian, S., Schatz, G. C. & Weiss, E. A. Energy transfer-enhanced photocatalytic reduction of protons within quantum dot light-harvesting–catalyst assemblies. *Proc. Natl Acad. Sci. USA* **115**, 8290–8295 (2018).
42. Jiang, Y., Wang, C., Rogers, C. R., Kodaimati, M. S. & Weiss, E. A. Regio- and diastereoselective intermolecular [2+2] cycloadditions photocatalysed by quantum dots. *Nat. Chem.* **11**, 1034–1040 (2019).
43. Yuan, Y.-P. et al. Improving photocatalytic hydrogen production of metal–organic framework UiO-66 octahedrons by dye-sensitization. *Appl. Catal. B Environ.* **168–169**, 572–576 (2015).
44. Tian, J. et al. Supramolecular metal-organic frameworks that display high homogeneous and heterogeneous photocatalytic activity for H_2 production. *Nat. Commun.* **7**, 11580 (2016).
45. Orazietti, M., Kuss-Petermann, M., Hamm, P. & Wenger, O. S. Light-driven electron accumulation in a molecular pentad. *Angew. Chem. Int. Ed.* **55**, 9407–9410 (2016).
46. Kuss-Petermann, M., Orazietti, M., Neuburger, M., Hamm, P. & Wenger, O. S. Intramolecular light-driven accumulation of reduction equivalents by proton-coupled electron transfer. *J. Am. Chem. Soc.* **139**, 5225–5232 (2017).
47. Cardona, T., Sedoud, A., Cox, N. & Rutherford, A. W. Charge separation in photosystem II: a comparative and evolutionary overview. *Biochim. Biophys. Acta* **1817**, 26–43 (2012).
48. Congreve, D. N. et al. External quantum efficiency above 100% in a singlet-exciton-fission–based organic photovoltaic cell. *Science* **340**, 334–337 (2013).
49. Lee, J., Jadhav, P. & Baldo, M. A. High efficiency organic multilayer photodetectors based on singlet exciton fission. *Appl. Phys. Lett.* **95**, 033301 (2009).
50. Kim, J. H., Hansora, D., Sharma, P., Jang, J.-W. & Lee, J. S. Toward practical solar hydrogen production – an artificial photosynthetic leaf-to-farm challenge. *Chem. Soc. Rev.* **48**, 1908–1971 (2019).
51. Ardo, S. et al. Pathways to electrochemical solar-hydrogen technologies. *Energy Environ. Sci.* **11**, 2768–2783 (2018).
52. Foster, S. L. et al. Catalysts for nitrogen reduction to ammonia. *Nat. Catal.* **1**, 490–500 (2018).
53. Appel, A. M. et al. Frontiers, opportunities, and challenges in biochemical and chemical catalysis of CO_2 fixation. *Chem. Rev.* **113**, 6621–6658 (2013).
54. Can, M., Armstrong, F. A. & Ragsdale, S. W. Structure, function, and mechanism of the nickel metalloenzymes, CO dehydrogenase, and acetyl-CoA synthase. *Chem. Rev.* **114**, 4149–4174 (2014).
55. Kung, Y. & Drennan, C. L. in *The Biological Chemistry of Nickel* Ch. 7 (eds Zamble, D., Rowińska-Żyrek, M. & Kozlowski, H.) 121–148 (Royal Society of Chemistry, 2017).
56. Smith, P. T., Nichols, E. M., Cao, Z. & Chang, C. J. Hybrid catalysts for artificial photosynthesis: merging approaches from molecular, materials, and biological catalysis. *Acc. Chem. Res.* **53**, 575–587 (2020).
57. Kung, Y., Doukov, T. I., Seravalli, J., Ragsdale, S. W. & Drennan, C. L. Crystallographic snapshots of cyanide- and water-bound C-clusters from bifunctional carbon monoxide dehydrogenase/acetyl-CoA synthase. *Biochemistry* **48**, 7432–7440 (2009).
58. Heo, J., Halbleib, C. M. & Ludden, P. W. Redox-dependent activation of CO dehydrogenase from *Rhodospirillum rubrum*. *Proc. Natl Acad. Sci. USA* **98**, 7690–7693 (2001).
59. Lin, S. et al. Covalent organic frameworks comprising cobalt porphyrins for catalytic CO_2 reduction in water. *Science* **349**, 1208–1213 (2015).
60. Baek, J. et al. Bioinspired metal–organic framework catalysts for selective methane oxidation to methanol. *J. Am. Chem. Soc.* **140**, 18208–18216 (2018).
61. Handoko, A. D., Wei, F., Jenndy, Yeo, B. S. & Seh, Z. W. Understanding heterogeneous electrocatalytic carbon dioxide reduction through operando techniques. *Nat. Catal.* **1**, 922–934 (2018).
62. Hall, A. S., Yoon, Y., Wuttig, A. & Surendranath, Y. Mesostructure-induced selectivity in CO_2 reduction catalysis. *J. Am. Chem. Soc.* **137**, 14834–14837 (2015).
63. Yoon, Y., Hall, A. S. & Surendranath, Y. Tuning of silver catalyst mesostructure promotes selective carbon dioxide conversion into fuels. *Angew. Chem. Int. Ed.* **55**, 15282–15286 (2016).
64. Zhuang, T.-T. et al. Copper nanocavities confine intermediates for efficient electrosynthesis of C3 alcohol fuels from carbon monoxide. *Nat. Catal.* **1**, 946–951 (2018).
65. Raugei, S. et al. Experimental and computational mechanistic studies guiding the rational design of molecular electrocatalysts for production and oxidation of hydrogen. *Inorg. Chem.* **55**, 445–460 (2016).
66. Helm, M. L., Stewart, M. P., Bullock, R. M., DuBois, M. R. & DuBois, D. L. A synthetic nickel electrocatalyst with a turnover frequency above 100,000 s^{-1} for H_2 production. *Science* **333**, 863–866 (2011).
67. Li, W. et al. A bio-inspired coordination polymer as outstanding water oxidation catalyst via second coordination sphere engineering. *Nat. Commun.* **10**, 5074 (2019).
68. Ung, G. & Peters, J. C. Low-temperature N_2 binding to two-coordinate L_2Fe^0 enables reductive trapping of $L_2FeN_2^-$ and NH_3 generation. *Angew. Chem. Int. Ed.* **54**, 532–535 (2015).
69. Lee, Y., Mankad, N. P. & Peters, J. C. Triggering N_2 uptake via redox-induced expulsion of coordinated NH_3 and N_2 silylation at trigonal bipyramidal iron. *Nat. Chem.* **2**, 558–565 (2010).
70. Costentin, C., Drouet, S., Robert, M. & Savéant, J.-M. A local proton source enhances CO_2 electroreduction to CO by a molecular Fe catalyst. *Science* **338**, 90–94 (2012).
71. Schmeier, T. J., Dobereiner, G. E., Crabtree, R. H. & Hazari, N. Secondary coordination sphere interactions facilitate the insertion step in an iridium(III) CO_2 reduction catalyst. *J. Am. Chem. Soc.* **133**, 9274–9277 (2011).
72. Haviv, E. et al. A thiourea tether in the second coordination sphere as a binding site for CO_2 and a proton donor promotes the electrochemical reduction of CO_2 to CO catalyzed by a rhenium bipyridine-type complex. *J. Am. Chem. Soc.* **140**, 12451–12456 (2018).
73. Chapovetsky, A. et al. Pendant hydrogen-bond donors in cobalt catalysts independently enhance CO_2 reduction. *ACS Cent. Sci.* **4**, 397–404 (2018).
74. Nichols, E. M., Derrick, J. S., Nistanaki, S. K., Smith, P. T. & Chang, C. J. Positional effects of second-sphere amide pendants on electrochemical CO_2 reduction catalyzed by iron porphyrins. *Chem. Sci.* **9**, 2952–2960 (2018).
75. Azcarate, I., Costentin, C., Robert, M. & Savéant, J.-M. Through-space charge interaction substituent effects in molecular catalysis leading to the design of the most efficient catalyst of CO_2-to-CO electrochemical conversion. *J. Am. Chem. Soc.* **138**, 16639–16644 (2016).
76. Han, Z., Kortlever, R., Chen, H.-Y., Peters, J. C. & Agapie, T. CO_2 reduction selective for $C_{\geq 2}$ products on polycrystalline copper with N-substituted pyridinium additives. *ACS Cent. Sci.* **3**, 853–859 (2017).
77. Jiao, Y., Zheng, Y., Chen, P., Jaroniec, M. & Qiao, S.-Z. Molecular scaffolding strategy with synergistic active centers to facilitate electrocatalytic CO_2 reduction to hydrocarbon/alcohol. *J. Am. Chem. Soc.* **139**, 18093–18100 (2017).
78. Liu, M. et al. Enhanced electrocatalytic CO_2 reduction via field-induced reagent concentration. *Nature* **537**, 382–386 (2016).
79. Li, Y. H., Liu, P. F., Li, C. & Yang, H. G. Sharp-tipped zinc nanowires as an efficient electrocatalyst for carbon dioxide reduction. *Chem. Eur. J.* **24**, 15486–15490 (2018).
80. Hammes-Schiffer, S. Proton-coupled electron transfer: moving together and charging forward. *J. Am. Chem. Soc.* **137**, 8860–8871 (2015).
81. Hammes-Schiffer, S. Theory of proton-coupled electron transfer in energy conversion processes. *Acc. Chem. Res.* **42**, 1881–1889 (2009).
82. Kai, T., Zhou, M., Duan, Z., Henkelman, G. A. & Bard, A. J. Detection of $CO_2^{\bullet-}$ in the electrochemical reduction of carbon dioxide in *N*,*N*-dimethylformamide by scanning electrochemical microscopy. *J. Am. Chem. Soc.* **139**, 18552–18557 (2017).
83. Mondal, B., Song, J., Neese, F. & Ye, S. Bio-inspired mechanistic insights into CO_2 reduction. *Curr. Opin. Chem. Biol.* **25**, 103–109 (2015).
84. Jackson, M. N., Pegis, M. L. & Surendranath, Y. Graphite-conjugated acids reveal a molecular framework for proton-coupled electron transfer at electrode surfaces. *ACS Cent. Sci.* **5**, 831–841 (2019).
85. Jackson, M. N. et al. Strong electronic coupling of molecular sites to graphitic electrodes via pyrazine conjugation. *J. Am. Chem. Soc.* **140**, 1004–1010 (2018).
86. Cai, R. & Minteer, S. D. Nitrogenase bioelectrocatalysis: from understanding electron-transfer mechanisms to energy applications. *ACS Energy Lett.* **3**, 2736–2742 (2018).
87. Milton, R. D. et al. Bioelectrochemical Haber–Bosch process: an ammonia-producing H_2/N_2 fuel cell. *Angew. Chem. Int. Ed.* **56**, 2680–2683 (2017).
88. Yuan, M. & Minteer, S. D. Redox polymers in electrochemical systems: From methods of mediation to energy storage. *Curr. Opin. Electrochem.* **15**, 1–6 (2019).
89. Li, Y. C. et al. Electrolysis of CO_2 to syngas in bipolar membrane-based electrochemical cells. *ACS Energy Lett.* **1**, 1149–1153 (2016).
90. Salvatore, D. A. et al. Electrolysis of gaseous CO_2 to CO in a flow cell with a bipolar membrane. *ACS Energy Lett.* **3**, 149–154 (2017).
91. Bakker, J. G. C., Van Grondelle, R. & Den Hollander, W. T. F. Trapping, loss and annihilation of excitations in a photosynthetic system: II. Experiments with the purple bacteria *Rhodospirillum rubrum* and *Rhodopseudomonas capsulata*. *Biochim. Biophys. Acta* **725**, 508–518 (1983).
92. Gillbro, T., Sandström, Å., Spangfort, M., Sundström, V. & van Grondelle, R. Excitation energy annihilation in aggregates of chlorophyll ab complexes. *Biochim. Biophys. Acta* **934**, 369–374 (1988).
93. Hashimoto, H., Sugai, Y., Uragami, C., Gardiner, A. T. & Cogdell, R. J. Natural and artificial light-harvesting systems utilizing the functions of carotenoids. *J. Photochem. Photobiol. C Photochem. Rev.* **25**, 46–70 (2015).
94. Barzda, V. et al. Singlet–singlet annihilation kinetics in aggregates and trimers of LHCII. *Biophys. J.* **80**, 2409–2421 (2001).
95. Geacintov, N. E., Breton, J., Swenberg, C. E. & Paillotin, G. A single pulse picosecond laser study of exciton dynamics in chloroplasts. *Photochem. Photobiol.* **26**, 629–638 (1977).
96. Haedler, A. T. et al. Long-range energy transport in single supramolecular nanofibres at room temperature. *Nature* **523**, 196–199 (2015).
97. Krueger, B. P., Scholes, G. D. & Fleming, G. R. Calculation of couplings and energy-transfer pathways between the pigments of LH2 by the ab initio transition density cube method. *J. Phys. Chem. B* **102**, 5378–5386 (1998).
98. Caram, J. R. et al. Room-temperature micron-scale exciton migration in a stabilized emissive molecular aggregate. *Nano Lett.* **16**, 6808–6815 (2016).
99. Li, J.-J., Chen, Y., Yu, J., Cheng, N. & Liu, Y. A supramolecular artificial light-harvesting system with an ultrahigh antenna effect. *Adv. Mater.* **29**, 1701905 (2017).
100. Scholes, G. D., Fleming, G. R., Olaya-Castro, A. & van Grondelle, R. Lessons from nature about solar light harvesting. *Nat. Chem.* **3**, 763–774 (2011).
101. Sim, M. et al. Dependence of exciton diffusion length on crystalline order in conjugated polymers. *J. Phys. Chem. C* **118**, 760–766 (2014).
102. Mikhnenko, O. V. et al. Exciton diffusion length in narrow bandgap polymers. *Energy Environ. Sci.* **5**, 6960–6965 (2012).
103. Cui, Y. et al. Organic photovoltaic cell with 17% efficiency and superior processability. *Natl. Sci. Rev.* **7**, 1239–1246 (2019).
104. Scholes, G. D. Long-range resonance energy transfer in molecular systems. *Annu. Rev. Phys. Chem.* **54**, 57–87 (2003).
105. Förster, T. Zwischenmolekulare energiewanderung und fluoreszenz. *Ann. Phys.* **437**, 55–75 (1948).
106. Scholes, G. D., Jordanides, X. J. & Fleming, G. R. Adapting the Förster theory of energy transfer for modeling dynamics in aggregated molecular assemblies. *J. Phys. Chem. B* **105**, 1640–1651 (2001).
107. Medintz, I. L. & Hildebrandt, N. *FRET - Förster Resonance Energy Transfer: From Theory to Applications* (Wiley, 2013).

108. Cnops, K. et al. 8.4% efficient fullerene-free organic solar cells exploiting long-range exciton energy transfer. *Nat. Commun.* **5**, 3406 (2014).
109. Gupta, V., Bharti, V., Kumar, M., Chand, S. & Heeger, A. J. Polymer–polymer Förster resonance energy transfer significantly boosts the power conversion efficiency of bulk-heterojunction solar cells. *Adv. Mater.* **27**, 4398–4404 (2015).
110. Mohapatra, A. A. et al. Förster resonance energy transfer drives higher efficiency in ternary blend organic solar cells. *ACS Appl. Energy Mater.* **1**, 4874–4882 (2018).
111. Xu, W.-L. et al. Förster resonance energy transfer and energy cascade in broadband photodetectors with ternary polymer bulk heterojunction. *J. Phys. Chem. C* **119**, 21913–21920 (2015).
112. Feron, K. et al. Utilizing energy transfer in binary and ternary bulk heterojunction organic solar cells. *ACS Appl. Mater. Interfaces* **8**, 20928–20937 (2016).
113. Nam, M. et al. Long-term efficient organic photovoltaics based on quaternary bulk heterojunctions. *Nat. Commun.* **8**, 14068 (2017).
114. Kramer, I. J., Levina, L., Debnath, R., Zhitomirsky, D. & Sargent, E. H. Solar cells using quantum funnels. *Nano Lett.* **11**, 3701–3706 (2011).
115. Baek, S.-W. et al. Efficient hybrid colloidal quantum dot/organic solar cells mediated by near-infrared sensitizing small molecules. *Nat. Energy* **4**, 969–976 (2019).
116. Quintero-Bermudez, R. et al. Ligand-induced surface charge density modulation generates local type-II band alignment in reduced-dimensional perovskites. *J. Am. Chem. Soc.* **141**, 13459–13467 (2019).
117. Proppe, A. H. et al. Synthetic control over quantum well width distribution and carrier migration in low-dimensional perovskite photovoltaics. *J. Am. Chem. Soc.* **140**, 2890–2896 (2018).
118. Cao, D. H., Stoumpos, C. C., Farha, O. K., Hupp, J. T. & Kanatzidis, M. G. 2D homologous perovskites as light-absorbing materials for solar cell applications. *J. Am. Chem. Soc.* **137**, 7843–7850 (2015).
119. Giebink, N. C., Lassiter, B. E., Wiederrecht, G. P., Wasielewski, M. R. & Forrest, S. R. Ideal diode equation for organic heterojunctions. II. The role of polaron pair recombination. *Phys. Rev. B* **82**, 155306 (2010).
120. Schlenker, C. W. et al. Cascade organic solar cells. *Chem. Mater.* **23**, 4132–4140 (2011).
121. Nikolis, V. C. et al. Reducing voltage losses in cascade organic solar cells while maintaining high external quantum efficiencies. *Adv. Energy Mater.* **7**, 1700855 (2017).
122. Cnops, K., Rand, B. P., Cheyns, D. & Heremans, P. Enhanced photocurrent and open-circuit voltage in a 3-layer cascade organic solar cell. *Appl. Phys. Lett.* **101**, 143301 (2012).
123. Gasparini, N., Salleo, A., McCulloch, I. & Baran, D. The role of the third component in ternary organic solar cells. *Nat. Rev. Mater.* **4**, 229–242 (2019).
124. Wang, C. et al. Ternary organic solar cells with enhanced open circuit voltage. *Nano Energy* **37**, 24–31 (2017).
125. Lu, L., Xu, T., Chen, W., Landry, E. S. & Yu, L. Ternary blend polymer solar cells with enhanced power conversion efficiency. *Nat. Photonics* **8**, 716–722 (2014).
126. Gasparini, N. et al. Designing ternary blend bulk heterojunction solar cells with reduced carrier recombination and a fill factor of 77%. *Nat. Energy* **1**, 16118 (2016).
127. Schwarze, M. et al. Impact of molecular quadrupole moments on the energy levels at organic heterojunctions. *Nat. Commun.* **10**, 2466 (2019).
128. Schwarze, M. et al. Band structure engineering in organic semiconductors. *Science* **352**, 1446–1449 (2016).
129. Arias-Rotondo, D. M. & McCusker, J. K. The photophysics of photoredox catalysis: a roadmap for catalyst design. *Chem. Soc. Rev.* **45**, 5803–5820 (2016).
130. Ebbesen, T. W. Hybrid light–matter states in a molecular and material science perspective. *Acc. Chem. Res.* **49**, 2403–2412 (2016).
131. Thomas, A. et al. Tilting a ground-state reactivity landscape by vibrational strong coupling. *Science* **363**, 615–619 (2019).
132. Thomas, A. et al. Ground-state chemical reactivity under vibrational coupling to the vacuum electromagnetic field. *Angew. Chem. Int. Ed.* **128**, 11634–11638 (2016).
133. Ruggenthaler, M. et al. Quantum-electrodynamical density-functional theory: bridging quantum optics and electronic-structure theory. *Phys. Rev. A* **90**, 012508 (2014).
134. Tokatly, I. V. Time-dependent density functional theory for many-electron systems interacting with cavity photons. *Phys. Rev. Lett.* **110**, 233001 (2013).
135. Flick, J. & Narang, P. Cavity-correlated electron-nuclear dynamics from first principles. *Phys. Rev. Lett.* **121**, 113002 (2018).
136. Flick, J. & Narang, P. Excited-state nanophotonic and polaritonic chemistry with ab initio potential-energy surfaces. Preprint at *arXiv* https://arxiv.org/abs/1907.04646 (2019).
137. Costentin, C. & Nocera, D. G. Self-healing catalysis in water. *Proc. Natl Acad. Sci. USA* **114**, 13380–13384 (2017).
138. Yang, Y. & Urban, M. W. Self-healing polymeric materials. *Chem. Soc. Rev.* **42**, 7446–7467 (2013).
139. Ricca, E., Brucher, B. & Schrittwieser, J. H. Multi-enzymatic cascade reactions: overview and perspectives. *Adv. Synth. Catal.* **353**, 2239–2262 (2011).
140. Hickey, D. P., Gaffney, E. M. & Minteer, S. D. Electrometabolic pathways: recent developments in bioelectrocatalytic cascades. *Top. Curr. Chem.* **376**, 43 (2018).
141. Cazelles, R. et al. Reduction of CO_2 to methanol by a polyenzymatic system encapsulated in phospholipids–silica nanocapsules. *New J. Chem.* **37**, 3721–3730 (2013).
142. Lum, Y. & Ager, J. W. Sequential catalysis controls selectivity in electrochemical CO_2 reduction on Cu. *Energy Environ. Sci.* **11**, 2935–2944 (2018).
143. Deng, Y. & Yeo, B. S. Characterization of electrocatalytic water splitting and CO_2 reduction reactions using in situ/operando Raman spectroscopy. *ACS Catal.* **7**, 7873–7889 (2017).
144. Luna, P. D. et al. Catalyst electro-redeposition controls morphology and oxidation state for selective carbon dioxide reduction. *Nat. Catal.* **1**, 103–110 (2018).
145. Genovese, C. et al. Operando spectroscopy study of the carbon dioxide electro-reduction by iron species on nitrogen-doped carbon. *Nat. Commun.* **9**, 935 (2018).
146. Luo, J. et al. A compact tunable polarized X-ray source based on laser-plasma helical undulators. *Sci. Rep.* **6**, 29101 (2016).
147. Maurizio, C., Rovezzi, M., Bardelli, F., Pais, H. G. & D'Acapito, F. Setup for optimized grazing incidence x-ray absorption experiments on thin films on substrates. *Rev. Sci. Instrum.* **80**, 063904 (2009).
148. Young, I. D. et al. Structure of photosystem II and substrate binding at room temperature. *Nature* **540**, 453–457 (2016).
149. Kern, J. et al. Simultaneous femtosecond X-ray spectroscopy and diffraction of photosystem II at room temperature. *Science* **340**, 491–495 (2013).
150. Kupitz, C. et al. Serial time-resolved crystallography of photosystem II using a femtosecond X-ray laser. *Nature* **513**, 261–265 (2014).
151. Göttle, A. J. & Koper, M. T. M. Proton-coupled electron transfer in the electrocatalysis of CO_2 reduction: prediction of sequential vs. concerted pathways using DFT. *Chem. Sci.* **8**, 458–465 (2017).
152. Brockherde, F. et al. Bypassing the Kohn-Sham equations with machine learning. *Nat. Commun.* **8**, 1872 (2017).
153. Čorić, I., Mercado, B. Q., Bill, E., Vinyard, D. J. & Holland, P. L. Binding of dinitrogen to an iron–sulfur–carbon site. *Nature* **526**, 96–99 (2015).
154. Rodriguez, M. M., Bill, E., Brennessel, W. W. & Holland, P. L. N_2 reduction and hydrogenation to ammonia by a molecular iron-potassium complex. *Science* **334**, 780–783 (2011).
155. Gómez-Bombarelli, R. et al. Design of efficient molecular organic light-emitting diodes by a high-throughput virtual screening and experimental approach. *Nat. Mater.* **15**, 1120–1127 (2016).
156. Granda, J. M., Donina, L., Dragone, V., Long, D.-L. & Cronin, L. Controlling an organic synthesis robot with machine learning to search for new reactivity. *Nature* **559**, 377–381 (2018).
157. Ahneman, D. T., Estrada, J. G., Lin, S., Dreher, S. D. & Doyle, A. G. Predicting reaction performance in C–N cross-coupling using machine learning. *Science* **360**, 186–190 (2018).
158. Scheuring, S. & Sturgis, J. N. Chromatic adaptation of photosynthetic membranes. *Science* **309**, 484–487 (2005).
159. Bahatyrova, S. et al. The native architecture of a photosynthetic membrane. *Nature* **430**, 1058–1062 (2004).
160. McDermott, G. et al. Crystal structure of an integral membrane light-harvesting complex from photosynthetic bacteria. *Nature* **374**, 517–521 (1995).
161. Sundström, V., Pullerits, T. & van Grondelle, R. Photosynthetic light-harvesting: reconciling dynamics and structure of purple bacterial LH2 reveals function of photosynthetic unit. *J. Phys. Chem. B* **103**, 2327–2346 (1999).
162. Zheng, X. et al. Theory-driven design of high-valence metal sites for water oxidation confirmed using *in situ* soft X-ray absorption. *Nat. Chem.* **10**, 149–154 (2018).

Acknowledgements
All authors acknowledge support from CIFAR for facilitating meetings that helped conceive this work and related collaborations. C.J.C. thanks DOE/LBNL grant 101528-002 for funding. G.S.-C., A.G.D. and G.D.S acknowledge support from the Division of Chemical Sciences, Geosciences, and Biosciences, Office of Basic Energy Sciences of the U.S. Department of Energy through grant no. DE-SC0019370. A.H.P. was partly funded through a CGS D grant from NSERC. We thank Fraser Armstrong, Barry Rand, Koen Vandewal and Johannes Benduhn for helpful discussions.

Author contributions
All authors contributed to the discussion of content. A.H.P. and Y.C.L. gathered content and wrote the initial draft, with input from all co-authors. All authors helped revise the manuscript before submission.

Competing interests
The authors declare no competing interests.

Publisher's note
Springer Nature remains neutral with regard to jurisdictional claims in published maps and institutional affiliations.